Free Flow Acoustophoresis

Technology Transfer from Silicon to Glass

Axel Tojo

November, 2012

LUND UNIVERSITY

Master's Thesis

Faculty of Engineering, LTH
Department of Measurement Technology and
Industrial Electrical Engineering
Division of Electrical Measurements

Supervisors: Carl Grenvall, Johan Nilsson

There is a theory which states that if ever anyone discovers
exactly what the Universe is for and why it is here, it will instantly disappear
and be replaced by something even more bizarre and inexplicable.
There is another theory which states that this has already happened.

– Douglas Adams –

Acknowledgements

First of all I would like to thank my supervisor Calle. I send my thanks to my co-supervisor Johan Nilsson for being a true leader and prefekt, for caring about his personnel and to my examinator Thomas Laurell for being an inspirational head of research.

I am of course also hugely in dept to everyone else at the department for Measurement Technology and Industrial Electrical Engineering (Elmät) for their support, encouragement and good times. My thanks go out to Belinda for fun collaboration on green spots and letting me in on my first article. To John for always having time to chat and for solving my Matlab problems. To Monica for truly putting value on education. To Christian for letting me borrow his "super glue". To Per for everything from making amplifiers to helping me with loops. To Martin for eating most and fastest. To Magnus for trusting me to concoct the pacemaker exercise. To Andreas C for teaching me why flash ADC are never more than 8-bit. To Fredrik E for letting me be the opponent for his thesis and for pushing me to finish. To Simon for entertaining us with burning snowballs. To Mikael for all good discussions and for being passionate about bread. To Eva for fixing all that other stuff engineers don't really want to bother with. To Maria E for never understanding my fascination with layers. To Johan G for good teaching collaborations and furniture moving. To Björn for good exchanges of ideas. To Ola for all crazy stuff and for basically introducing me to everything at Elmät. To Tomas J for letting me borrow his crayons. To Désirée for all collaborations on the courses and pushing me to finish writing this thesis, I hope I haven't made your life too difficult. To Andreas L for fixing BMC access for everyone. To Malgorzata for giving me the parents perspective on children abroad, it made me appreciate my parents in law even more. To Lennart N improving all my constructions and being an anti-chaos champion. To Tobias for many a good lunch walks and talks. To Maria N for teaching me all about the Coulter Counter. To Pelle for also pursuing all possible leads. To Hans W P for highlighting the dangers of bureaucracy. To Klara for teaching me about Korea. To Elly for good discussions during seminar breaks; keep on dancing. To Josefin for working on awesome stuff, like dolphins and equality. To Maria T for giving me a chance to test my matlab skills. To Valle for bringing me to Elmät in the first place and updating my pass card a gazillion times. To Ulrika for eloquently shouldering the role of Eva, continuing to make our lives run smoothly. To Hong for many interesting discussions on the Chinese and Japanese language and for the 月饼.

My thanks also goes out to all of my dual family in Sweden and Japan, you are all awesome. Last, though foremost, this thesis is dedicated to my lovely wife Naoko and son Takeo. にゃああ！

Table of contents

List of Abbreviations

AC	Alternating Current
DNA	Deoxyribo Nucleic Acid
DRIE	Deep Reactive Ion Etch
EOF	Electro-Osmotic Flow
FFA	Free Flow Acoustophoresis
HF	HydroFluoric acid
IC	Integrated Circuit
MEMS	MicroElectroMechanical Systems
NIL	NanoImprint Lithography
PIV	Particle Image Velocimetry
PRF	Primary Radiation Force
PS	PolyStyrene
PZT	Lead Zirconate Titanate
RBC	Red Blood Cell
RIE	Reactive Ion Etch
RTP	Room Temperature and Pressure
SRF	Secondary Radiation Force
TATP	TriAcetone TriPeroxide
USW	Ultrasonic Standing Wave
μTAS	Micro Total Analysis System

1 Introduction

1.1 Background

Everything started with mixing that went wrong in the deep, long-forgotten back waters of a distant planet, and so life arose on Earth. Fast forward. Some 3.7 billion years later a couple of engineering students got the task to use ultrasound to mix particles and a liquid within a small channel. To everyone's surprise they found that, instead of being mixed, the particles were aligned in well defined rows instead[1]. Since this was opposite to what they were trying to achieve the result was, much like life, regarded as a failure at the time.

Microfluidics is the field of science working with fluids (i.e. gases and liquids) in the microscale and below. Based on this loose definition the applications then range from basic particle manipulation and phase mixing to fully integrated systems such as ink jet printers and chemical sensors. This thesis concerns the technique called Free Flow Acoustophoresis (FFA), a separation method based on acoustic parameters (e.g. radius, density, compressibility etc.). From a standing ultrasound wave (USW) a force proportional to the radius cubed (or volume) acts on particles in a fluid. In a liquid the particle velocity thus becomes dependent on size (and other acoustic properties) which enables separation. This thesis aims to provide a full review of the manufacturing process of an FFA microfluidic chip along with the necessary theoretical background. Previously FFA chips have been made in silicon while this thesis has the ultimate aim of transferring this technology to glass[2,3].

Microfluidics has great relevance in today's (and for that matter tomorrow's) society. Everyday examples such as ink jet printers have already been mentioned but the vast majority of applications lie within biomedicine in form of sensors, reactors, injectors etc. Hospital care relies more and more heavily on clinical chemistry/biology and currently around 80% of the clinical decisions are made or confirmed with body sample testing while only constituting about 5% of the medical care budget in Skåne, Sweden[4,5]. These tools are used extensively to achieve higher reproducibility, sensitivity and automation.

A more specific application of an FFA chip would be for evaluation of cell response to drugs. The drug can be administered to a single cell population which is then separated based on size. This gives subpopulations at different stage of the cell cycle and the response can be monitored individually. Another use of the FFA technology would be to get more monodisperse selections from a particle manufacturing process. By accurately selecting narrow distributions more specific demands from customers can be met. Though the big future of FFA is perhaps as an integrated part of more complex microfluidic systems in need of separation.

1.2 Content of each chapter

In the subsequent chapters on theory (ch. 2 through 6) the concepts and fundamentals needed to understand the FFA technology are presented. An attempt has been made to arrange these chapters in a logical order, but the reader is of course free to choose whatever order based on previous knowledge and interest.

1.2.1 Chapter 2 – Micro fabrication

Fabrication of microfluidic chip derives most of its techniques and methods from integrated circuit (IC) technology, though the materials are not necessarily semiconductors. Glass is an interesting material due to favorable properties in terms of optics, inertia and heat behavior. Processing of glass to create channel devices follows a procedure of lithography, (wet) etching and bonding all described in this chapter.

1.2.2 Chapter 3 – Microfluidics

At the heart of microfluidics is laminar flow – the domain where all turbulent flows are absent. Thus no mixing within or between fluids occur except due to diffusion. To describe and predict laminar flow behavior several parameters are used such as Reynolds number, Péclet number, and hydraulic diameter. Another important concept is Stoke's drag which describes the friction force experienced by a particle moving in a fluid.

1.2.3 Chapter 4 – Wave theory and Sound

Sound waves are oscillations travelling through a medium, be it gas, liquid or solid. Due to the nature (or lack) of interconnections between atoms or molecules in liquids and gases only longitudinal motions are possible. Two waves coexisting at the same point in space and time will interfere with each other. If the two waves of the same frequency travel in opposite directions, either from two sources or reflection, a standing wave pattern of oscillating areas and displacement nodes emerges.

1.2.4 Chapter 5 – Acoustic Forces

In an acoustic wave field, as described in chapter 4, a force acts on particles suspended in the fluid medium. The expression for this force is related to certain properties of the particles as well as the medium and also the nature of the acoustic wave field. In terms of particle movement the acoustic force is balanced by Stoke's drag described in chapter 3. Other effects such as secondary forces from scattered sound and streaming from energy losses in the fluid are also mentioned.

1.2.5 Chapter 6 – Free Flow Acoustophoresis

Because particles move in a predictable manner due to the acoustic forces this technology can be used to create numerous devices. This thesis deals with a method called free flow acoustophoresis (FFA) where particles are sorted based (mainly) on

size. The basic principle, complications as well as certain enhancements are investigated in this chapter.

1.3 On the use of tau

Throughout this thesis I will use τ (= 6.28318…) as the circle constant relating radius to circumference. This is a much more natural and intuitive constant compared to customary π which relates diameter to circle circumference and numerous evidence and examples of this have been presented by Robert Palais and Michael Hartl[6,7]. Tau relates to pi simply as $\tau = 2\pi$. A small difference it might seem, though fundamental at its core. I do not believe this thesis will have any real significance in this matter, but it is a small step in the mathematical revolution to replace π with τ.

2 Micro fabrication

2.1 Glass vs. Silicon vs. Polymer

There are three distinct groups of materials available for microfluidic chip manufacturing: silicon (semiconductor), glass and plastics (polymer), each with their own advantages. Silicon was the first material used for microfluidic chip manufacturing based on the knowledge and methods gained from integrated circuit (IC) industry. Due to the crystal structure of silicon etching may be anisotropic which enables channel cross sections of a few different shapes. Most notably for resonance structures which is the main focus of this thesis silicon channels with square cross sections can be made. Though the anisotropic etching at the same limits channel construction to those planes and lines defined by the crystal structure. It would be possible to use other semiconductors, but they have no real advantage over silicon as the more advanced electrical properties of for instance gallium arsenide (GaAs) are rarely required in microfluidic systems. In addition the cost of silicon is significantly lower due to its availability.

Glass is the traditional and favored material of chemists, mostly for its inert properties and transparency. This obviously makes glass more suitable for optical measurements and experiments. Furthermore borosilicate glass (pyrex), which is most often used in chemistry, has a very low coefficient of thermal expansion making it resistant to thermal shock. The main benefit of glass is the simplified chip production process as it needs very little advanced fabrication equipment compared to silicon. In addition glass, due to its non-crystal nature, needs no mask alignment[8]. As is further described in chapter 2.4 the principal etching method available to glass is isotropic wet chemical etching. This enables the fabrication of any shape or structure which gives greater versatility and the possibility to avoid corner micro vortices.

Polymer-based chips have been growing quickly in recent years with the availability of easy fabrication methods at low cost. A difference to silicon and glass is that polymers can be permeable to liquids and gases. In applications involving acoustics polymers are less suitable due to their high attenuation of sound[9] and low acoustic impedance. When considering a possible upscale fabrication of microfluidic devices polymer and glass hold an advantage over silicon.

Due to the larger scale structures integrated circuit manufacturing techniques yields too small amount of chips per batch. A more plausible alternative when working with amorphous materials is hot embossing or nanoimprint lithography (NIL) which has been demonstrated on both small and large structures with high aspect ratio for glass[10,11].

2.2 Glass chip fabrication process

Glass chip fabrication follows normal lithographic procedures for semiconductors with a few exceptions. Micro lithography includes a number of steps described in figure 2.1 to transfer the desired pattern to a wafer. Details of the important parts will be further explained in chapters 2.3 through 2.5.

First the glass substrate is coated with a very thin (in the vicinity of 20nm) chromium layer. On top of the metal layer the photoresist is deposited through spin coating. The reason for depositing an extra chrome layer is to improve the adhesive power of the photoresist which might release if attached directly onto glass. The photoresist is then exposed either through UV-lithographic methods or (as is the case in this thesis) with a laser. Exposed resist is then prone to be removed by special solvent creating the desired pattern in the resist. For the etching fluid to reach the glass the chrome is also removed in the exposed areas. The pattern is then transferred from the mask to the glass substrate by etching with hydrofluoric acid (HF). After etching the remaining photoresist and chrome is removed and finally the structure is bonded to a clean glass plate creating sealed channels.

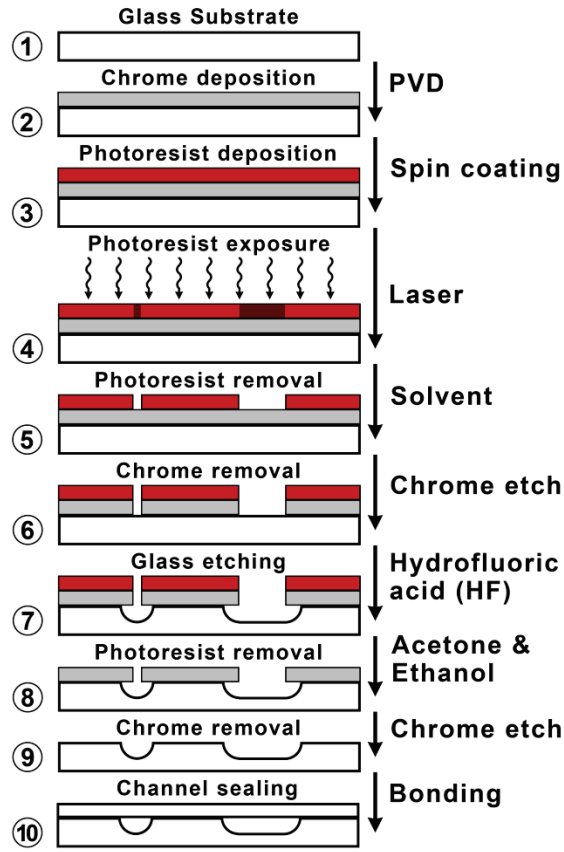

Figure 1 - Glass channel micro fabrication procedure. [a]

Lithography is particularly sensitive to dust and particles because these, if on the mask, will obstruct exposure and thereby change the pattern. Micro lithography must thus be performed in clean room environment, with higher class the smaller structures are to be made.

Quality of a lithography method is typically evaluated from three criteria[12]:

- *Resolution* – the minimum size of structure that can be fabricated with correspondence to the original mask.
- *Registration* – how well subsequent structures can be added with good matching.
- *Throughput* – rate of production.

2.3 Resists and Masking

The photoresist placed on the substrate is a polymer material sensitive to electro-magnetic radiation. Resists can be classified into two categories – positive and negative. In positive resists the radiation changes the chemical structure to make it soluble to certain developer fluids. Negative resists react opposite to this behavior – they are made from a polymer combined with a photosensitive substance. The latter component absorbs the energy initiating cross-linking of the polymer and subsequently makes the resist insoluble to the developer. Negative resists have a tendency to swell due to absorption of the developer fluid which limits the resolution.

Photoresists are most commonly deposited by spin-coating where a drop of resist is put in the center of the wafer which thereafter is spun so that the resist is evenly distributed. The thickness of the resist layer is determined by (the inverse of the) resist viscosity and rotation speed (squared). After spin-coating the wafer is baked to evaporate superfluous dissolving agent.

The structures required for free flow acoustophoresis are in the regime of a hundred micrometers and above and therefore no advanced masking techniques are necessary. Instead an etch mask is formed by directly exposing the resist with a laser.

2.4 Etching

2.4.1 General

Micro fabrication etching has evolved from its original 16th century art form, honed by masters of old such as Rembrandt, and the methods used today still follow very similar procedures. Etching methods can be divided into wet etching and dry etching techniques; the latter, including various forms of plasma etch and reactive ion etching (RIE), are outside the scope of this thesis. There are mainly two general methods of wet chemical etching. Either the entire substrate is submerged in a chemical solution or the etchant is continually sprayed onto the wafer surface. The glass etching described in this thesis involves only the bathing version.

Proper etching technique is crucial, not least in integrated circuit industry, to ensure that etching is uniform over the entire wafer as well as between different wafers and from batch to batch. The wet etch mechanism involves three steps[13,14]:

- Transport of etchant to the substrate surface
- Chemical interactions with the surface
- Transport of products away from surface

All three steps can limit the etch rate (which also depends on pressure, temperature and etchant agitation).

2.4.2 Isotropic & anisotropic etching

What differentiates iso- and anisotropic etching is whether a method etches at the same rate in all directions or not. The rate of anisotropy (A_f) is described according to equation (2.1) below

$$A_f = 1 - \frac{L}{H_f} \tag{2.1}$$

Where H_f is the vertical etch depth and L is the horisontal distance etched underneath the mask. One of the problems (or benefits?) of glass is that it is only possible to etch isotropically due to its amorphous nature.

As an isotropic etch will give an under-etch this must be taken into account in mask design. The desired channel dimensions will determine mask width (x) according to equation (2.2) and figure 2.2.

$$x = w - 2d \tag{2.2}$$

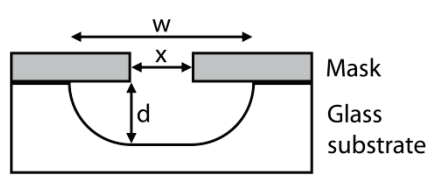

Figure 2 - Isotropic etching. The desired depth (d) and width (w) of the structure determines what mask width (x) needs to be used. [a]

2.4.3 Etch stop

An important part of etching is how to bring the process to a halt. Precision is essential, particularly when space is limited such as for integrated circuits, when a certain aspect ratio is desired or (as is the case in this thesis) when mechanical resonance is sought. For semiconductor etching there are a number of different etch-

stop techniques. In crystal materials the internal bonds are stronger or weaker in different directions and etch rates will follow accordingly. The dense 111-plane will etch slowly while the 110-plane etch rate is 16 times higher and for the 100-plane one hundred times higher[15]. Etch rates can also be affected by (deliberate or natural) impurities in the material.

Boron etch stop utilizes the slower etch rate in boron-doped silicon and can be used to create etch stop layers[16]. The PN-etch is an electro chemical etch technique where p-doped silicon is etched while n-doped is not. Therefore the n-doped silicon can be used both as a mask and to create etch stop layers[17,18]. However, the most simple etch stop method is time. Since the etch rate of a certain chemical, when properly mixed, is constant the desired etch depth can be reached through time calculations. This is the only approach readily available when working with glass and is the method solely used in this thesis.

2.5 Bonding

Bonding of glass-to-glass is not as readily done as is glass-to-silicon through anodic bonding[19,20]. The general method is to thoroughly clean wafers with sulphuric acid[21], piranha wash (se chapter 0) or similar procedures[19] and then simply bring the ultra clean surfaces together allowing van-der-Waals bonds to form. This part is very sensitive to dust or other particles and must therefore be performed in a clean room environment. In recent years it has been suggested that the bonding is better done submerged or in running water to avoid contamination[22,21]. To cement the linking the chip can be postprocessed through baking and pressure treatment. The drawback is that the weights used often leaves the glass surface roughened and "misty". Development seems to go towards low temperature bonding and various methods such as HF-fusion[23] and calcium-enhanced bonding[21] have been suggested.

3 Microfluidics

3.1 General

Microfluidics is the science and technology dealing with fluids and flows in the range of microliters (10^{-6}) and as far down as femto liters (10^{-18}). Though much of the theory already existed it was not until S.C. Terry constructed a miniature gas chromatograph in 1975 using integrated circuit technology[24] that microfluidics emerged in any practical sense. Development further continued in molecular analysis and with the boom of genomics in the 1980s[25]. Recent focus on proteomics and life science is only increasing the need of microfluidic solution for dispensing, cleaning, mixing and separation.

The first reason for using microfluidics would be when handling of very small liquid volumes is demanded (though on the opposite end problems concerning low throughput can arise). Further advantages include reduced liquid consumption which can be desirable when expensive chemicals are used (use efficiency) and for chemical reactions small volumes might increase safety if the reaction is strongly exothermic for instance. An additional effect is faster response times which come with shorter diffusion distances. Examples of microfluidic devices are ink jet printers, drug research and production, chemo-analytical systems etc. One of the main goals in microfluidic research is to go towards efficient automation with several functions on the same chip – often called micro total analysis system (μTAS) or lab-on-a-chip.

The field of microfluidics is too vast to cover in a single chapter, both concerning fundamentals as well as applications and this chapter will focus solely on issues of interest for FFA technology.

3.2 What is a fluid?

Fluids include both liquids and gases. The more formal definition of a fluid is "a substance which deforms continuously under the application of shear (tangential) stress, no matter how small that stress may be"[26]. Or to quote the legendary martial arts master Bruce Lee "You put it [water] in a teapot – it becomes the teapot"[27].

To simplify mathematical treatment certain subgroups can be extinguished. A Newtonian fluid is a fluid whose strain versus stress rate is linear and passes through the origin. Another way of expressing it is that the viscosity does not change with the strain rate applied to the fluid. This is a valid assumption for many liquids such as water.

3.3 Fluid mechanics

3.3.1 Laminar flow

Laminar flow is the opposite of turbulent flow. In the macro world liquids tend to mix naturally, like milk in a cup of tea. However under certain conditions, often fulfilled in microscale systems, two fluids coming into a common channel will instead laminate as seen in figure 3.1. The only mixing between the fluids is due to diffusion.

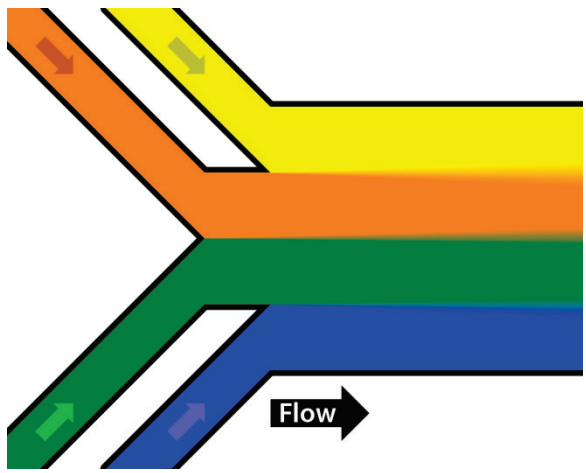

Figure 3 - Laminar flows does not mix like most fluids in the macro world, but laminates and retains their relative positions in the structure. The only mixing is due to diffusion at the fluid-fluid interfaces. [a]

3.3.2 Reynolds number

As laminar flow is a key factor of many microfluidic applications it is interesting to be able to determine whether laminar flows are to be expected or not. The Reynolds number (*Re*) is a factor used for this purpose. The equation for calculating the Reynolds number is

$$Re = \frac{\rho D_{\mathrm{h}} u}{\eta} \tag{3.1}$$

Where ρ is the density of the liquid, u the average velocity, D_{h} the hydraulic diameter of the channel described in chapter 3.3.3 and η is the dynamic (absolute) viscosity. The transition from laminar to turbulent flow occurs in the region of $Re = 2000$ in both the macro and the micro domain[28]. The exact threshold varies dependent on such factors as channel shape, aspect ratio and surface roughness[29]. As an example a rectangular channel of 375 x 150 µm flowing with water at a rate of 100 µl/min would have a Reynolds number of 7. Well into the laminar domain.

Yet another region is found at values of $Re << 1$ which is called Stokes flow or creeping flow[30,28]. In this case the advective inertial forces (fluid bulk momentum) will be small compared to the viscous forces. Thus the flows are what can be called truly laminar and follow edges or other structures (hence creeping) without forming vortices. Mathematically all time dependency will disappear and the flow is completely time reversible[31], except for diffusion which is not part of the (Navier-Stokes) model.

Laminar flows are not however, as it might seem, restricted to microscale systems. Indeed this condition is dependent on the factors given in equation 3.1 - flow velocity, hydraulic diameter, viscosity and density of the liquid - and can occur even in huge macroscale systems. A very good example of this is the glacier streams on Greenland which can be seen in figure 3.2. Particularly at junctions some part of the flow picks up earth, sand or gravel. This dark stained snow retain its relative position all the way down to the ocean due to the laminar flow. Though the dimensions of the stream are large the viscosity of the packed snow is large enough and the velocity low enough to create a laminar flow even in this case.

Figure 4 - Streams of packed snow running down from Greenland glaciers to the Atlantic ocean. Dark earth or gravel stained snow retain its relative position in the flow all the way down to the ocean. Despite the large dimensions the flow is laminar due to the low velocity and high viscosity of the snow.[b]

3.3.3 Hydraulic diameter

In most cases the channels in microfluidic systems are not circular as is common in macro systems. Instead the cross section is dependent on etch method as shown in chapter 2.4. The hydraulic diameter (D_h) can be used to approximate the flow for arbitrary geometries.

$$D_h = \frac{4 \cdot cross\ section\ area}{wetted\ perimeter} = \frac{4A}{P_{wet}} \tag{3.2}$$

With a completely filled channel the wetted perimeter is the perimeter of the channel cross-section. The hydraulic diameter should be used to calculate the radius in Poisseuille's law when channel cross-section is not circular.

3.3.4 Pressure Flow and Flow profiles

Most microfluidic systems use pressure driven flows. These systems can be evaluated with fluid circuit theory, utilizing terminology and ideas from electrical circuits. The pressure (P) can be seen as the potential of the system and flow (Q) is equivalent to current. Fluidic resistance (R), binding pressure to flow as per Ohm's law, is then derived from Poiseuilles law[32,33], or the Hagen-Poiseuilles equation as it is also known

$$R = \frac{16\eta L}{\tau r^4} \tag{3.3}$$

In equation (3.3) η is the dynamic viscosity, L is the length of the channel and r is the radius of a circular channel. For other channel geometries the hydraulic diameter should be used. The analogy to electrical systems can be taken even further to model both capacitance symbolizing hydraulic compliance as well as hydraulic inductance or the ability of a system to maintain a given flow[34] (current) through these things lie outside the scope of this thesis.

When a Newtonian fluid goes through a microchannel it will be subject to what is called a no-slip condition at the solid-fluid interface (i.e the flow rate will be zero closest to the walls)[35]. Consequently the flow velocity will be at maximum at the center of the channel. This leads to a parabolic velocity profile across the channel according to equation –

$$v(d) = \frac{\Delta P}{4\eta L} \cdot (r^2 - d^2) \tag{3.4}$$

where d is the distance from the channel wall and r is the channel radius. More complex expressions are needed if channel cross-section are not circular[1]. For this thesis however, it is enough to note that the parabolic flow profile will behave

approximately according to equation (3.4) across the shortest side while taking on a more blunt appearance across the longest side of the channel.

Another popular method is electro-osmotic flow (EOF) which enables movement of liquid containing ions. A polar liquid, such as water, will give a contacting surface a charge[36]. This in turn will create a so called diffuse layer of ions of the opposite charge. When an electrical potential is applied to the column, with an anode at one end of the column and a cathode at another, the ions of the diffuse layer will migrate towards the appropriate electrode. Since these ions are solved and clustered along the walls of the channel, they drag the rest of the solution with them, even the anions of opposite charge. The resulting flow profile will be quite flat in the entire channel apart from the diffuse layer.

3.3.5 Entrance effects

When a fluid enters a micro channel from a large scale connection the laminar flow does not develop immediately due to differences in flow profiles. A macro channel would, at least seen from a micro channel point of view, have a uniform velocity profile whereas the no-slip conditions in the micro channel will create a parabolic flow as discussed in chapter 3.3.4. Based on appropriate hydraulic diameter (D_h) and Reynolds number (Re) equation (3.5) describes an estimation of the length needed to establish the flow profile[37].

$$\frac{L_e}{D_h} = \frac{0.6}{1 + 0.035 \cdot Re_{D_h}} + 0.056 \cdot Re_{D_h} \tag{3.5}$$

For the example channel in chapter 3.3.2 this would give an entrance length of about 90 μm. The equation for the entrance length is still an approximation as the exact value will depend on the precise geometries of the connecting channels and the interface.

Though entrance effects should be considered the microfluidic chips in this thesis uses tube connections of micrometer size (300 μm in diameter) which ought to even further reduce the actual entrance length. In addition the FFA uses a prefocus channel, further explained in chapter 6.3; any disturbance of the flow before or early in this part should have negligible effects on performance.

3.4 Diffusion

In the absence of turbulent flows mixing occurs mainly through diffusion in the laminar domain. Diffusion is the net transport of molecules due to random particle movement [29] which can be seen as the somewhat blurred interface between liquids in figure 3.2. However it is important to note that the random movement of the fluid particles occurs in the entire volume, not only at the interface.

Figure 5 - The only mixing in a laminar flow is due to diffusion which here can be seen through the creation of a gradient when different fluids are led into the same channel. [a]

Generally diffusion is described by Fick's law of diffusion (equation 3.6).

$$\frac{\partial}{\partial t}c(\bar{x},t) = D\nabla^2 c(\bar{x},t) \tag{3.6}$$

The equation has different interpretation dependent of application. In the case of particle diffusion c is the concentration as a function of space and time[38]. In his landmark paper in 1905 Einstein derived the diffusion coefficient D as[39]

$$D = \frac{RT}{fN_{\mathrm{A}}} \tag{3.7}$$

$$D = \frac{k_{\mathrm{B}}T}{3\tau\eta a} \tag{3.8}$$

where R the gas constant, T the absolute temperature, N_{A} Avogadro's number and f the friction factor proportional to the viscosity η. The partial differential equation that is Fick's law describes the relationship between the change in concentration and its derivative. Diffusion, however, is based on the random movements of particles where the position of a particle can not be correlated to a previous position in time or space. Fick's law must thus be seen as a completely statistical conclusion of the bulk behavior of a system with many such particles[38].

A more practical formula is the Einstein-Smoluchowski equation derived from the diffusion equation which gives the time τ_{D} it takes for a particle to travel a distance d

$$\tau_{\mathrm{D}} = \frac{d^2}{2D} \tag{3.9}$$

3.5 Stokes' Drag

An important expression when calculating forces on suspended particles is Stokes' drag which comes from solving the Navier-Stokes equation in the laminar flow regime[40]. Stokes' law will give the fluid resistance force (F_{drag}) acting on a moving particle and is expressed as

$$F_{\mathrm{drag}} = 3\tau\eta a_{\mathrm{p}} v \tag{3.10}$$

Where η is the viscosity, a_p the particle radius and v its velocity. This force has traditionally been used to estimate the terminal velocity of falling particles but in this thesis it is used, balanced by the acoustic radiation force (chapter 0), to calculate traveling distance of cells and beads. As noted above Stokes' law is only valid for single particles at Reynolds numbers below one. However, this is the Reynolds number local to the particle, not necessarily corresponding to the over-all value of the channel as calculated in chapter 3.3.2[41]. The matter will be further investigated in chapter 5.4 when Stokes' drag is balanced by acoustic forces.

4 Wave theory and Sound

4.1 Sound Waves

Sound is a wave of particle vibrations travelling through matter. It is important to note that while the wave travels forward it does not create any transport of material as each individual atom or molecule only oscillates around its resting point. The wave does however transport energy[42]. Depending on how the medium atoms or molecules are coupled different types of waves can arise - transversal and longitudinal. Transversal waves are waves with movement perpendicular to the propagation direction, for example the snake-like movement of a whip or the strings of a guitar. In longitudinal waves the movement is in the same direction as the propagation such as in a Newton's cradle. Both longitudinal and transversal waves can propagate through solid materials while gases and liquids only can hold longitudinal waves. As this thesis mainly deals with fluids only longitudinal waves will be considered henceforth. The theory and equations governing the two types are, however, practically identical. The hyperbolic partial differential equation as seen in equation (4.1) is the general equation governing a wave *s* in the one dimension

$$\frac{\partial^2 s}{\partial t^2} = \frac{1}{v^2}\frac{\partial^2 s}{\partial x^2} \tag{4.1}$$

where *t* is time, *v* the wave velocity and *x* the position. There are many solutions to this well established equation though for the scope of this thesis it is enough to consider the most basic (and common) form described in equation (4.2).

$$s(x,t) = A \cdot \sin\left[\tau\left(\frac{t}{T} - \frac{x}{\lambda}\right) + \alpha\right] \tag{4.2}$$

A sound wave propagates as compressions and rarefactions and the wave can therefore also be expressed as in equation (4.3) and (4.4) as variations in gauge pressure (*p*).

$$p(x,t) = p_0 \cdot \cos\left[\tau\left(\frac{t}{T} - \frac{x}{\lambda}\right) + \alpha\right] \tag{4.3}$$

$$p_0 = B \cdot k \cdot A \tag{4.4}$$

P_0 is the gauge pressure amplitude, B the adiabatic bulk modulus and A the displacement amplitude from equation (4.2). Note that phase constant (α) is the same between the two equations though the pressure wave is phase shifted 90º to the displacement wave.

4.2 Standing Waves and Resonance

Wave interference can be calculated by simple superposition. A special case is standing waves, which arises when two identical waves, traveling in opposite directions, meet. Equation (4.5) describes a standing wave and comes by adding and rearranging two waves as described to equation (4.2) but with differing signs for the position factor due to direction.

$$s_{sw} = s_1 + s_2 = 2A \cdot \sin\left(\tau\frac{x}{\lambda} + \alpha\right) \cdot \cos\left(\tau\frac{t}{T} + \alpha\right) \tag{4.5}$$

The result is that equation (4.5) has one function dependent on position and one on time. If the phase shift (α) is temporarily ignored for a general case the position function will always be zero at an interval of half a wavelength. Thus the total wave exhibits stationary points called displacement nodes (DN) alternating with antinodes (DA) every quarter of a wavelength. Illustrated in figure 4.1 is a standing wave resonance of one and a half wavelength reflected against denser media (described below). The same expression can be calculated for the pressure wave

$$p(x,t) = -2p_0 \cdot \cos\left(\tau\frac{x}{\lambda} + \alpha\right) \cdot \cos\left(\tau\frac{t}{T} + \alpha\right) \tag{4.6}$$

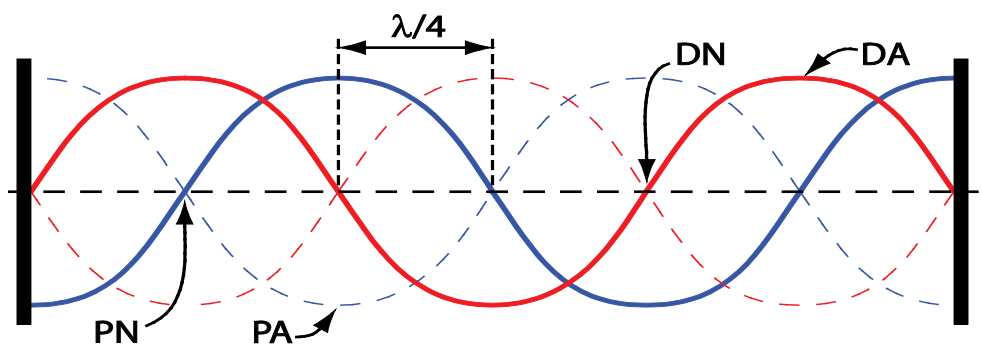

Figure 6 - Standing wave resonance of one and a half wave length. The red sine wave represents the pressure oscillations and the blue wave the displacement behaviour. The two are phase shifted 90º to each other, though they are of course only two sides of the same phenomenon. [c]

Comparing equation 4.5 with 4.4 the pressure and displacement functions are 90º out of phase with respect to position, but not time. This means a pressure node (PN) is always positioned at a displacement antinode and vice versa[1]. A standing wave like exampled above may arise from two sources or from one source and reflection. Depending on the media (or rather its acoustic impedance *Z*) at the reflection boundary the wave will change its phase α. If the outer media, as seen outside the "wall" in figure 4.1, has an acoustic impedance lower than the inner media the displacement wave will have an antinode at the boundary. In this thesis the inner

media is, for all intents and purposes, water and the outer media is glass which have Z=10^6 and Z=10^7 respectively[43]. Thus the displacement wave will instead have a node at the boundary as seen in figure 4.1. To fulfill this criterion the phase change is

$$\alpha = 0 + n\frac{\tau}{2} \qquad where\ n \in \mathbb{Z} \tag{4.7}$$

where $\mathbb{Z}$ is an integer.

4.3 Ultrasound & Piezoelectric Actuators

The human hearing ranges (ideally) from 20 Hz to 20 kHz and everything below is called infrasound while everything above goes by the name of ultrasound. Due to higher forces achieved at higher frequencies (further explained in chapter 0) this thesis deals only with ultrasound in the range of megahertz.

To generate sound waves of these frequencies piezoelectric actuators are used. Simply put piezoelectricity is the coupling between mechanical and electrical behaviour. A material with this property will deform when a voltage is applied and vice versa will polarise under mechanical stress. The piezoelectric effect arises from a non-centrosymmetric charge distribution in the crystal unit cell. A deformation of the material changes the bond angles and thus also the charge distribution giving a net polarisation. Some materials exhibit piezoelectricity naturally (e.g. quartz) though most are synthesized crystals such as PZT (lead zirconate titanate) and Rochelle salt. The mentioned three materials have an transformation efficiency of 0.01, 0.52 and 0.81 respectively[44].

Piezoelectric materials thus convert electrical energy to mechanical energy or the other way around with fairly high efficiency. This is beneficial for example in transducers for diagnostic ultrasound where piezo-electric elements can be used both to generate pulses and to read the response echo[45]. By applying an alternating current (AC) to a piezoelectric material it will expand at negative voltage and contract at positive voltage thus producing an oscillation of the same frequency as the electrical signal. The actor plate must however be designed with a certain frequency range in mind as it will vibrate most strongly at its resonance frequency which corresponds to a thickness of half a wavelength[45,46].

5 Acoustic Forces

5.1 Primary Radiation Force

When a sound wave traveling through a liquid media encounters a particle of different physical properties than the surrounding substance it will experience a net force (primarily) in line with the wave. The force arises due to the difference in density and compressibility between the particle and its surrounding medium which alters the speed of sound and subsequently the oscillation pattern. Particles under the influence of a progressive wave experience only a negligible force. However, in the case of a stationary sound wave field the radiation pressure rises significantly[47].

First described by King in 1934[47] and later Yoshioka and Kawashima, Gor'kov and others the behavior of the acoustic primary radiation force (PRF) has been thoroughly investigated. Several system factors control the magnitude of the acoustic force. Apart from the mentioned density and compressibility (ρ and β respectively) other influential parameters are the pressure amplitude (P), particle radius (a), wavelength (λ) and position in the wave field ($2ky$) – all gathered in equation (5.1) as denoted by Gor'kov[34,48] below.

$$F_r = 2\tau a^2(ka) \cdot E_{ac} \cdot \phi(\beta, \rho) \cdot sin(2ky) \tag{5.1}$$

This equation can be divided into four distinctive parts as seen in equation (5.1) separated by multiplication signs. These parts are further explained in chapter 5.2. In all subsequent equations the parameters originating from the medium uses the subscript 0 (zero) and those concerning the particles use a.

5.2 Breakdown of the Force Equation

5.2.1 Pre-factor

The pre-factor collects miscellaneous system parameters not fitting the other categories below. Most notably, and of particular interest in this thesis, the PRF is highly dependent on particle size. An example of two particles is given in figure 5.1, being at the same position the larger particle experience a larger force due to its radius. Acoustic forces arise due to scattering of the sound wave at the particle boundary[34] which introduces the surface area as a parameter. Particle radius also affects in the ka(=τa/λ) term that relates the particle size to wavelength. Note that a shorter wave length (i.e. higher frequency) yields a larger force – a primary benefit of microscale systems.

An alternative way to write the pre-factor would be to break out the radius from the size-to-wavelength ratio and use particle volume [49,29].

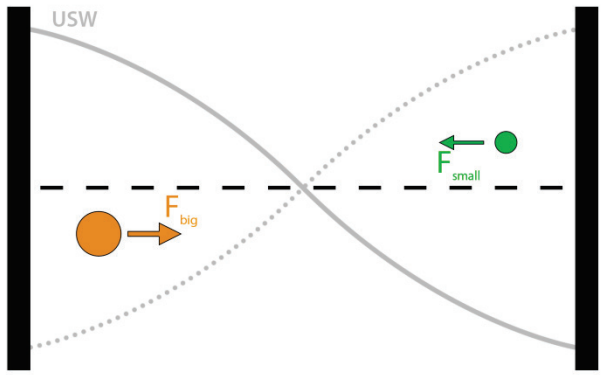

Figure 7 - The PRF acting on a particle is dependent on the radius (cubed). Thus two particles of different size, positioned at equal distance from the pressure node, will have different amount of force acting on them. The larger particle (orange) will experience a stronger force while the smaller particle will experience a (relatively) weaker force. [a]

5.2.2 Energy factor

E_{ac} is the energy density of the standing wave (equation (5.2)). Quite intuitively the energy scales with the sound wave pressure amplitude (P) squared and is coupled with the compressibility (β) of the medium. Compressibility relates the volume change of a material per unit of pressure applied and can be calculated (at a specific temperature) from its density and the speed of sound in the material.

$$E_{\mathrm{ac}} = \frac{P^2}{4\rho_0 c_0^2} = \frac{P^2 \cdot \beta_0}{4} \tag{5.2}$$

5.2.3 Acoustic contrast factor

Investigated by Kawashima and Yoshioka in 1955 the acoustic contrast factor (φ - eq. (5.3)) solves the force dependence on the relationship between density and compressibility of the particle and its' medium[50].

$$\phi = \frac{\rho_{\mathrm{a}} + \frac{2}{3}(\rho_{\mathrm{a}} - \rho_0)}{2\rho_{\mathrm{a}} + \rho_0} - \frac{1}{3}\frac{\beta_0}{\beta_{\mathrm{a}}} \tag{5.3}$$

As can be seen in equation (5.3) the dominant density will determine the sign of the contrast factor and thus the direction of the PRF. Though slightly simplified, the consequence of this is that a particle of a material denser than the surrounding medium will move towards the pressure nodes whereas a particle with lower density

will move in the opposite direction (i.e. to the pressure antinodes) as described in figure 5.2. A practical example is the separation of blood fats[51]. Under the influence of a USW red blood cells will move into the pressure nodes while any components "lighter" than plasma, such as lipid particles, will be shifted towards the pressure antinodes.

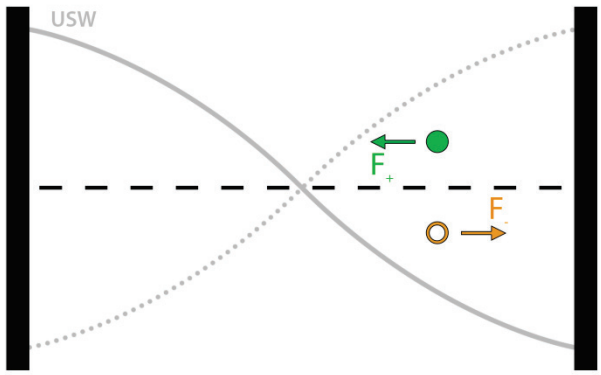

Figure 8 - Particles with a contrast factor of different signs will move in opposite directions when under influence of the PRF. The whole particle (green) has a positive contrast factor and will move towards the pressure node while the hollow particle (orange) has a negative factor and moves towards the pressure anti-node. [a]

5.2.4 Wave field position factor

Last in the force equation is $\sin(2ky)$ where $k = \frac{\tau}{\lambda} = \frac{\omega}{c}$ and y is the distance from a pressure node. This final factor expresses how much of the total force a particle will experience dependent on its' position in the wave field. Inside the sine function $\frac{y}{\lambda}$ will always give the particles' relative position as a fraction of the standing wave. In the case of a channel adjusted to half a wavelength (figure 5.3) the force distribution will reach maximum one quarter in from either side and have minima at the edges as well as in the center (figure 5.3).

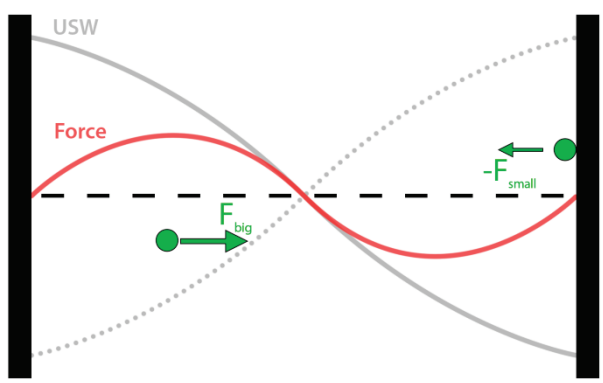

Figure 9 - The force acting upon particles is dependent on the position in the wave field. The PRF varies sinusoidally over the width of the channel with a period double to that of the resonance frequency of the USW. A particle located at one quarter of the channel width from the wall (orange) will experience maximal force. While a particle at the wall (green) or in the center will experience minimal force. [a]

5.3 Lateral forces

In addition to the horisontal component of the PRF described in chapter 5.2 there are lateral components acting to align particles along the pressure node though these forces are of minor significance in free flow acoustophoresis due to the continuous flow.

5.4 Stokes' drag revisited

In chapter 3.5 the fluid resistance or Stokes' drag was explained. This force is central as it is used in conjunction with the PRF to determine a particles position after a certain time and inversely the time it takes for a particle to reach a certain position. Stokes' law, however, is only valid far into the laminar domain. To ensure the use of Stokes' law is valid certain criteria must be fulfilled. In force balance calculations it is assumed that the inertia of the system is negligible[34]. In other words it is assumed that a particle reaches terminal velocity instantly when suddenly under the influence of an external force (F_{ext}). To verify this assumption the transient time of such a movement can be calculated for a spherical particle of radius *a* from a general force balance partial differential equation. The left side of the equation forms Newton's force equation of mass and acceleration which on the right side equals the sum of Stokes' drag and an external force which could be the acoustic force.

$$\frac{2}{3}\tau a^3 \rho \frac{\partial u}{\partial t} = -3\tau\eta a \cdot u + F_{\text{ext}} \tag{5.4}$$

Where ρ is the particle density, u its velocity and η the viscosity of the surrounding medium. By using integrating factor and a boundary condition of the sphere being at rest at $t = 0$ (ie. $u(0) = 0$) the velocity equation becomes

$$u(t) = \frac{F_{\text{ext}}}{6\eta\rho a}\left(1 - e^{-\frac{9\eta}{2\rho a^2}\cdot t}\right) \tag{5.5}$$

In equation (5.5) the first "1" is the (time independent) component of terminal velocity and the second part the velocity affected by acceleration. Looking at the characteristic time of the time dependent exponent, i.e. when

$$\frac{2\rho a^2}{9\eta} \cdot t = 1 \tag{5.6}$$

the transient time can be calculated. For a red blood cell with a density of 1125kg/m^3, a viscosity of 1 mPas (RTP) and a radius of 3.5 μm *t* is roughly 3μs. At such a short acceleration time it's reasonable to assume the particle reaches terminal velocity instantly.

Ignoring the acceleration of a suspended particle, is it valid to use Stokes' law? With the terminal velocity (u) from equation (5.7).

$$u = \frac{F_{\text{ext}}}{6\eta\rho a} \tag{5.7}$$

the local Reynolds number for the particle can be estimated from equation (3.1) as

$$Re = \frac{2\rho a}{\eta} \cdot u = \frac{F_{\text{ext}}}{3\eta^2} \tag{5.8}$$

using the particle radius a instead of the hydraulic diameter. The acoustic force acting on an erythrocyte at 3 MHz is roughly 2 pN[29] which yields a Reynolds number of about $6.7 \cdot 10^{-7}$, far below one as is required. Thus the use of Stokes' drag is valid.

5.5 Secondary radiation forces

It is well worth to notice the secondary radiation forces (SRF), particularly when dealing with high particle concentrations. A particle subject to an acoustic wave will act as a scatter source and nearby particles will be affected by this SRF according to equation (5.9)[52].

$$F_{\text{sr}} = 2\tau a^6 \left[\frac{\left(\rho_p - \rho_{\text{m}}\right)^2 (3\cos^2\theta - 1)}{6\rho_{\text{m}} d^4} v_{\text{m}}^2(x) - \frac{\omega^2 \rho_{\text{m}} \left(\beta_{\text{p}} - \beta_{\text{m}}\right)^2}{9d^2} p^2(x) \right] \tag{5.9}$$

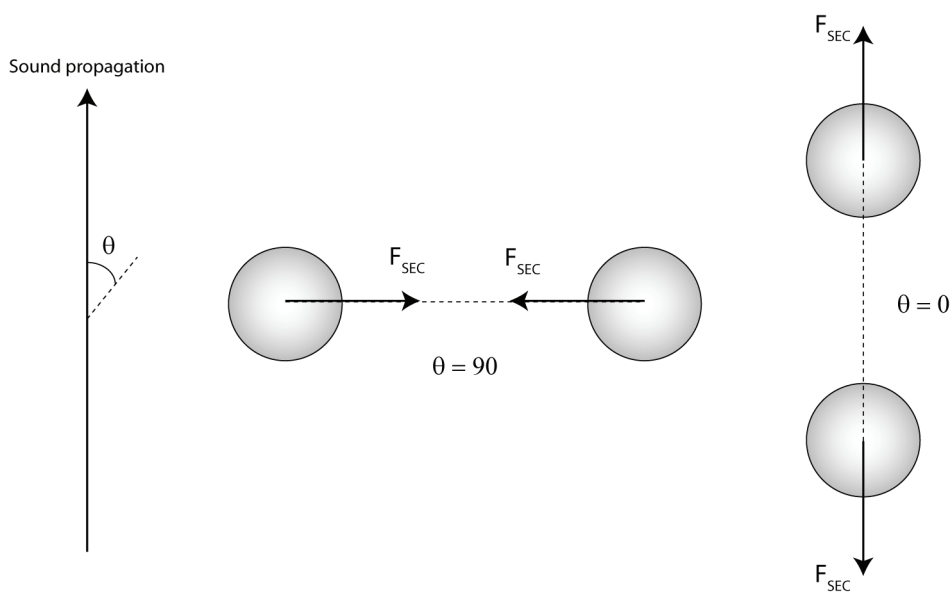

Figure 10 - The secondary radion force (SRF) arises due to scattered waves around the particle and is only relevant at very short distances. If two particles are positioned perpendicular to the sound propagation the SRF is attractive. While if the two particles are in line with the propagation the SRF is repulsive. [d]

where d is the center to center distance, θ is the angle between the center-to-center line and the primary wave propagation direction as seen in figure 5.4, $\omega = k \cdot c_a$, v(x) and p(x) are the velocity and pressure fields at the position of the particles. A negative sign denotes an attractive force.

The first important thing to notice is the strong dependence of interparticle distance (*d*) and particle radius (*a*). In the micro domain particle size will reduce the impact of the SRF; furthermore the strong inverse relationship with the distance between particles makes the SRF relevant only at very short distances. The first term is angle dependent so that when both particles are aligned perpendicular to the primary wave direction this part of the force becomes attractive and when the center to center line is parallel to the primary wave it is repulsive (figure 5.4). As the first part of the SRF is also related to velocity gradient of the medium it disappears when velocity reaches zero in the velocity nodes/pressure antinodes. The second part of the SRF is always attractive but will be reduced to zero in the pressure nodes where most dense particles will gather due to the PRF. Worth noting is also that the first term is dependent on compressibility while the second is dependent on density[53,54].

5.6 Acoustic streaming

Due to loss of acoustic energy through Reynold stresses, momentum is induced in the carrying medium. The result is called acoustic streaming and can be divided into three categories: Eckart streaming or Quartz wind, Rayleigh streaming and Schlichting streaming. Quartz wind is the basic streaming effect that appears as "vortex beams" originating from the sound center of the source according to figure 5.5. The acoustic wave will create a forward flow in the far field of the transducer[55]. When reaching an absorbing layer a proportion of the flow will be directed back towards the transducer, thus creating a vortex[56]. Streaming velocity scales with beam radius, e.g. transducer size which would reduce the effect for small transducers. Sizewise Eckart streaming acts on a length scale of several wavelengths and is therefore of minor interest in most microfluidic applications.

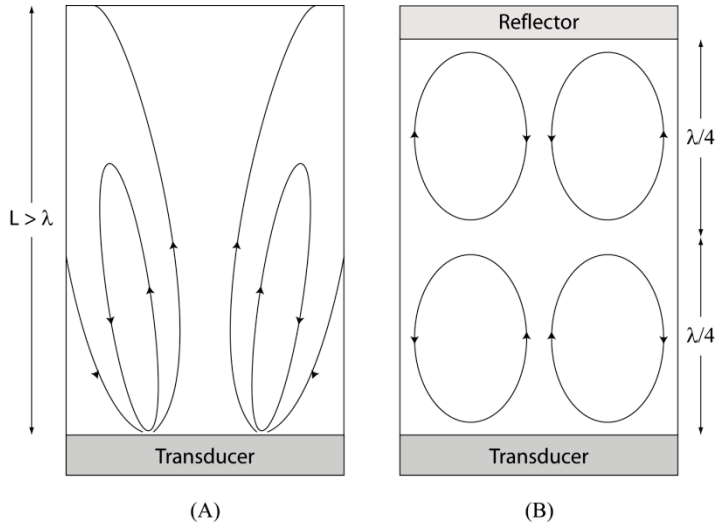

Figure 11 - A) Eckhart streaming creating a stream directed away from the center of the transducer. B) Rayleigh streaming with counter-rotating vortices spaced a quarter of a wavelength apart. Due to the similar resonance conditions Rayleigh streaming needs to be considered in acoustophoresis applications. [d]

The entire field of streaming was pioneered by Lord Rayleigh (John Strutt, 3d Baron Rayleigh) who observed vortices of quarter wavelength size in resonating fluid chambers[57]. Rayleigh streaming arises from the same effects as Quartz wind but the net behavior is different because of the altered movements in the standing wave field. Due to the similar resonance conditions, the effects of Rayleigh streaming should be considered in applications of acoustic microfluidics. For free flow acoustophoresis streaming effects are generally not desirable as they disrupt a controlled focus of particles. But streaming effects can be used to great benefit in mixing which is a hard task in microfluidics due to the laminar flows[58].

Schlichting streaming is seen as counter rotating vortices in the viscous boundary layer between the transducer and the Rayleigh vortices. Because of the small size the influence of Schlichting streaming is limited in the applications presented in this thesis[9].

6 Free Flow Acoustophoresis

6.1 Basic Separation Principle

The main topic of this thesis is free flow acoustophoresis – size based separation of particles through acoustic forces. Many other, more or less well known, "-phoresis" techniques exist. Foremost is electrophoresis where particles are separated under the influence of a static electric field. Most well known is perhaps the separation of DNA fragments in gel electrophoresis. The liquid containing DNA is placed at the edge of a porous (usually agar) gel. After the electric field is switched on the fragments will migrate towards the positive electrode because of the negative phosphor groups on DNA. Longer DNA strands are impeded in the agarose matrix and thereby move slower; over time the distance between segments of different length increase[59]. Other techniques work in analogous manner though based on different properties such as magnetism, thermal reaction[60] or, as in the case of acoustophoresis, radius, density, compressibility etc. as defined in equation 5.1.

6.2 One Dimensional FFA

Free Flow Acoustophoresis is a particle separation technique based mainly on two things: acoustic radiation force and laminar flows (see chapters 5.1-5.2 and 3.3.1 respectively). The first FFA was devised by Petersson et al.[2] and uses two particle inlets as seen in figure 6.1 (later models mostly include only a single inlet). The particles are led into the separation channel and laminated along the walls by a sheath flow. During their path through the separation channel the primary acoustic force

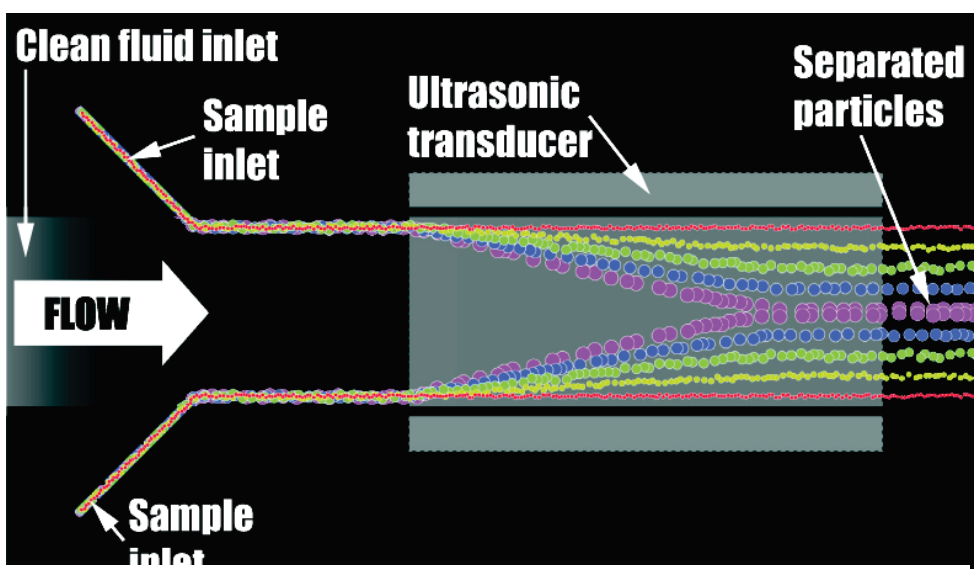

Figure 12 - Illustration of the basic FFA technology. Particles laminated against the walls are drawn towards the center of the channel due to the PRF, but move at different speed dependent on particle radius thus giving rise to a size gradient. [e]

acts perpendicular to the flow direction. With a half wave length resonance across the channel particles (of positive contrast factor) from both sides will move towards the pressure node corresponding to the middle of the channel. If otherwise similar, their velocity is determined by radius and acoustic propersties as described in chapter 5.1 which will form a particle gradient across the channel. Settings for optimal separation will depend on several factors, mainly the size distribution in the particle mix, particle contrast factors etc. The separated particles will hold their relative position in the channel due to the laminar flow. Each particle stream line can thus be extracted through its own outlet if flow rates are balanced appropriately.

This model has three major shortcomings. Using two particle inlets is good in that it utilizes the entire channel width. A perfectly symmetrical channel has, however, proven difficult to realize so that both particle streams reach optimal focus at the same time. Therefore this design has been replaced by a single sided chip. Second, the FFA-principle is based on all particles having a uniform starting position. This is only partly true and the width of the initial band is determined by the relationship between particle flow and sheath flow. Thus the lamination efficiency becomes coupled with overall flow speed which is not desirable. Third and last; due to the parabolic flow profile (see chapter 3.3.4) particles distributed along the vertical axis of the channel will have a varying retention time in the acoustic force field and therefore move different distance while in the separation channel, further enhancing the horisontal dispersion. It should be noted that most of these factors mentioned are coupled to each other which makes optimisation somewhat problematic.

6.3 2D FFA

To address these issues several enhancements can be made. In 2009 Grenvall et al.[3] introduced a prefocus step with a two dimensional acoustic force field as seen for a single sided chip in figure 6.2. By transporting all particles to the center of the inlet channel they will have a much more defined starting position once into the separation channel. To solve the problem of particles being freely distributed along the height of the channel the particles can simultaneously be focused along this axis.

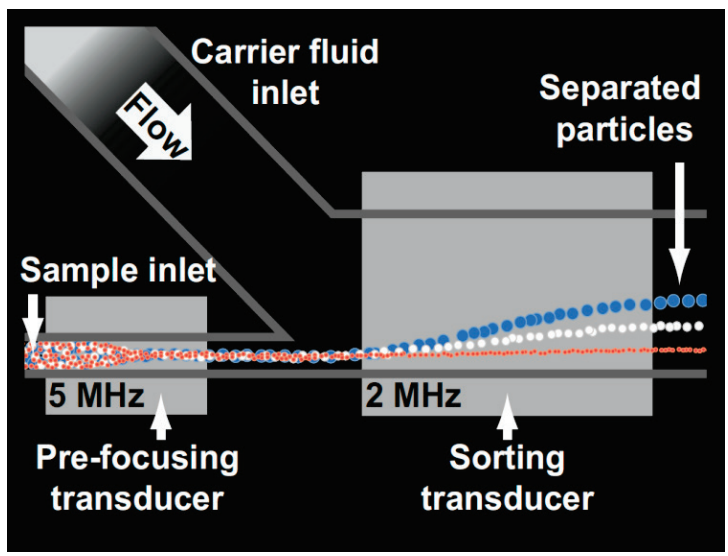

Figure 13 - Enhanced FFA with a two dimensional prefocus channel. The prefocus gives the particles a much more well defined starting position resulting in better separation. [f]

The prefocus channel is built to have a resonance frequency separate from the main channel to enable evaluation with and without prefocus. By constructing a square channel the same frequency (and thus the same transducer) can be used both for lateral and vertical focusing of particles. Other groups[61] have referred to the same technology as three-dimensional focusing. This does not make sense however as the focusing force field acts only in two planes, thus 2D-focusing, as a term, will be used in this thesis.

7 Methodology

7.1 Basic chip design

To create a FFA-chip in glass the obvious starting point is the 2D FFA design described in chapter 6.3 for a silicon chip. Certain limitations arise due to the new choice of material. Foremost is the unavailability of anisotropic etching (chapter 2.4.2) which makes it impossible to create a prefocus channel of different height from the main channel. A workaround, as seen in the figure 7.1, is to use the same two resonance frequencies in both main channel and prefocus channel. This will prevent the exclusion of the prefocus, but allows for the vertical focus to be turned off individually. A further benefit might be that particle streams in the main channel are also focused vertically, counteracting diffusion during separation compared to 1D FFA.

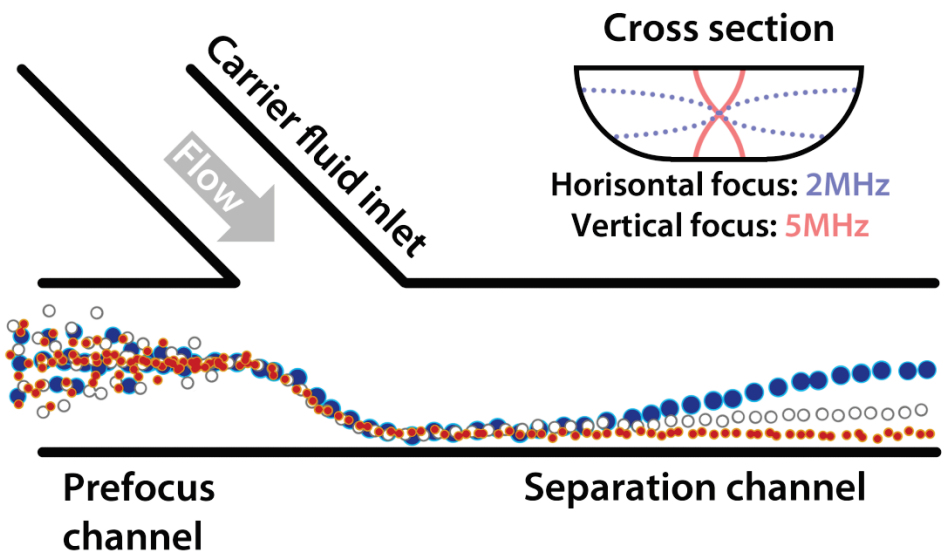

Figure 14 - FFA with two dimensional prefocus in glass. Cross section shows resonance conditions in the channel. The prefocus channel has been given the same dimensions as the separationchannel due to enable 2D focus despite the limitations of isotropic etching.

Particles are first focused to have a common starting point, then laminated against the wall. Finally in the separation channel the particles will move towards the center of the channel at a speed determined by their radius (and other acoustic properties). Larger particles will travel faster and thus reach the centerline first. [a]

The channel dimensions were etched to match 2 MHz horisontally and 5 MHz vertically which means 375 μm (at the widest part) and 150 μm respectively. To avoid undesired resonance the outlets and the sheath flow inlet are designed to avoid both frequencies present by adjusting their widths to 425 μm which relates to the main channel width by a factor of 1.13 and height by 2.83.

Diffusion can, as mentioned, be a major source of result degradation. To estimate the impact a review of the current chip design can be made. With a typical flow of 100μl/min at RTP the time spent in the main channel is 0.19s. Using the Einstein equation (3.7) and the Einstein-Smoluchowski equation (3.9) to calculate diffusion coefficient of a 5μm particle the diffusion distance is roughly 0.127μm or 2.5% of particle radius. This represents the average path travelled and rare particles might certainly travel longer though for these early experiments these numbers show it is safe to neglect diffusion.

7.2 Chips manufacture process

Most procedures in the chip manufacture process have been covered in chapter 2 while this chapter deals more with protocols and equipment used. All references to water in this chapter assume MilliQ grade water.

The wafers used were made from borofloat glass of 0.7 mm thickness prefabricated with a chromium layer and a positive resist layer on one side. Chromium is used to enhance adhesion between glass and resist. Pattern transfer was made directly on the wafer with a "DWL66 Laser Pattern Generator and Direct Writer" and afterwards developed with resist removal fluid (diluted "Microposit 351") for 60 seconds and chromium etch fluid for around 80 seconds.

Glass etching was done using a mix of concentrated hydrofluoric acid, nitric acid and water. Etch rate lies between 1-1.5 μm/minute and was calculated for each batch by microscope measurement after one hour of etching. To minimize and ease removal of glass shards access holes were drilled before the resist was removed with acetone and ethanol.

Before the bonding process the wafers were wiped with a clean room grade cloth and then chemically cleaned in near-boiling "Piranha wash" (concentrated sulphuric acid and hydrogen peroxide). Care was taken to remove all acetone before piranha wash as sulphuric acid, hydrogen peroxide and acetone forms triacetone triperoxide (TATP), a primary explosive extremely sensitive to shock and overall thermal decomposition[62,63].

Following the cleaning step wafers were thoroughly rinsed in multiple water baths and blow dried with nitrogen gas after which bonding was carried out by simply matching the plates and pressing them together by hand. To further enhance

bonding strength and suppress or remove voids the chip was annealed under pressure by weights in an "Evenheat CE Copper STP" glass oven at 500ºC.

Tube access connections were glued to the chip using silicon rubber (A07) from Wacker and the tubes used for all setups were Supelco Analytical Teflon tubing with 0.3, 0.5 or 0.8 mm inner diameter.

7.3 Experiment Setup

7.3.1 Overview

An overview of the experiment setup can be seen in figure 7.2. Centered around the FFA chip the equipment can be divided into an electrical part, a fluidic part and an evaluation (optical) part.

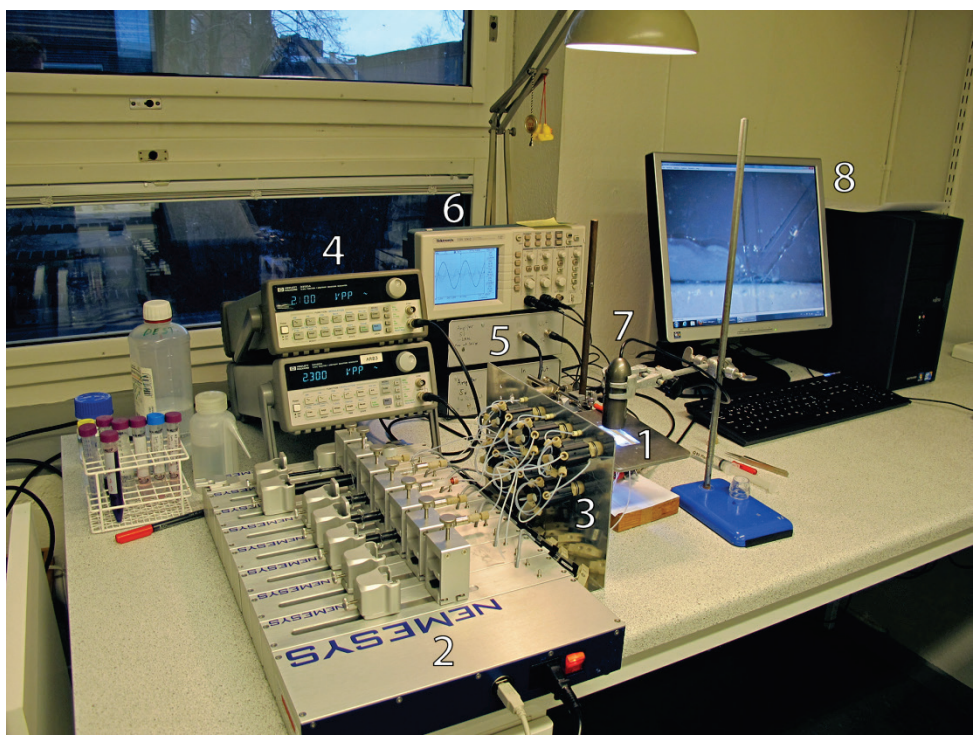

Figure 15 – An overview of the experiment setup used. [a]

1. FFA chip.
2. Syringe pump system (all inlet and outlet flows were controlled from here.
3. Rack of 100 µl loops used to collect samples.
4. Tone generators used to drive the transducers.
5. Amplifiers.
6. Oscilloscope.
7. Microscope and camera.
8. Computer

At the center of the set-up lies the chip itself. The USW was introduced through two piezoelectric transducers, one for each frequency (2 and 5 MHz). Those, in turn, were given their signal by two tone generators through in house amplifiers. The transducers were glued onto the chip and too small to be seen in figure 7.2.

Particle-, sheath and extraction flows were controlled by a single Nemesys pump system and 100 μl loops were used to collect samples from the outlets. To monitor the system a microscope connected to a computer was used. Several different microscopes and light sources were used though all were, from a practical viewpoint, equivalent. In figure 7.2 a USB-microscope is seen, but mostly a regular microscope with an external camera was used.

7.3.2 FFA chip setup

The full FFA chip can be seen in figure 7.3 with inlets, outlets and flow directions marked. The piezoelectric actuator sizes and positions are approximate.

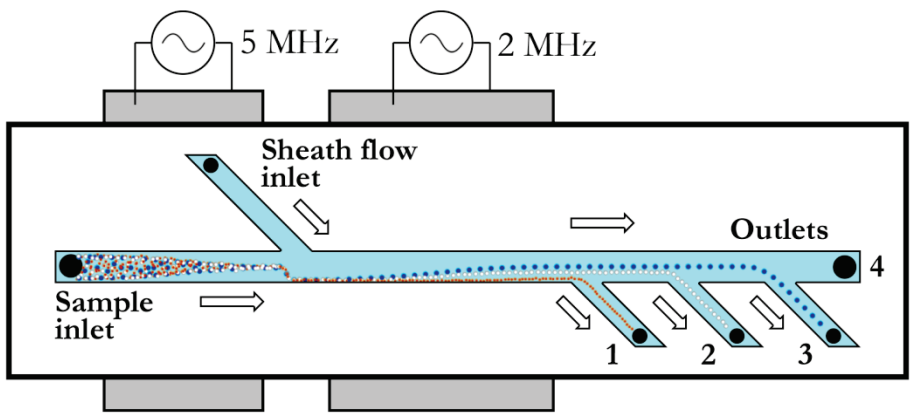

Figure 16 - Overview of the full FFA glass chip including piezoelectric actuators. Flow directions are indicated by arrows. [a]

As seen previously in chapter 7.1 particles are introduced through the sample inlet and focused in the first section. The particles are then pushed towards the wall by the sheath flow to start their separation run towards the center. Due to the laminar flow particles will retain their relative position in the channel after separation and can thus be led out through different outlets with appropriately adjusted flow rates.

The flow of both inlets as well as outlets 1-3, seen in figure 7.3, were run individually by syringe pumps. Outlet 4 was left open ended. Before starting experiments the entire flow system, including the chip, tubing, syringes, were filled with buffer to eliminate any air bubbles. Loops were cleaned both before and after experiments with milliQ multiple times to remove any remains and finally filled with air. To initiate experiments all the syringe pumps, tone generators, amplifiers etc. were

started and the system was left to stabilise before sample collection was started. Sinus signals were used to drive the piezoelectric actuators. Outlet flows were balanced each experiment to ensure each particle streamline exited through the correct outlet. During sample collection the loops were open long enough to fill them a couple of times.

After each run the samples were extracted from the loops into plastic microtubes for storage before analysis. Each sample was vortexed thoroughly and analysed in a Coulter Counter.

7.3.3 Specifications

Unless you are interested in the specific brands, chemicals and components this chapter can be skipped in favour of chapters 7.3.1 and 7.3.2 which explains the setup in a much more comprehensive and pleasant manner.

To induce the acoustic wave 2 MHz and 5 MHz piezo-electric elements (Pz26, Ferroperm Piezoceramics AS, Kvistgard, Denmark) were used. Both the main 2 MHz and the 5 MHz actuator were glued onto the chip with "Superglue" or more specifically Ethyl-2-cyanoacrylat (ExpressLim, Akzo Nobel Bygglim AB, Sweden). To generate the electrical signals two wave form generators (HP 3325B, Hewlett-Packard Inc., Palo Alto, CA, USA) and an in-house amplifier (based on LT1012, Linear Technology Corp., Milpitas, CA, USA) were used. The signal was monitored with an oscilloscope (TDS 1002, Tektronix UK Ltd., Bracknell, UK).

Tubing and access connections have already been described in the chip manufacture specifics (chapter 7.2). Further the fluidic system was driven by syringe pumps (Nemesys, Cetoni GmbH, Korbussen, Germany) using glass syringes (1001-10 TLL, Hamilton Bonaduz AG, Bonaduz, Switzerland). To capture fluid an analytical sample injector (7010, Rheodyne, Rohnert Park, CA, USA) set up with 100 μl loops were used.

For evaluation a Nikon microscope (SMZ-2T, Nikon, Tokyo, Japan) was lit with a Photonic PL2000 fiber optic lamp. Images and video were captured using a microscope fitted camera (EO-3112C, Edmund Optics Ltd, York, UK). Analysis of samples was made with a Coulter Counter (Multisizer 3, Beckman Coulter Inc., Fullerton, CA, USA).

All particles used for separation tests were plastic particles based on polystyrene (PS) (Sigma-Aldrich, Buchs SG, Switzerland). Samples were stored in 0.6 ml microtubes (MCT-060-L-C, Axygen inc., Union City, CA, USA).

8 Results

During the initial testing of the FFA-system only visual inspection was done to verify the separation process and images showing the particles in different stream lines can be seen in figure 8.1.

The first sample measurements were made separating a blend of 3 μm and 7 μm particles. Presented in figure 8.2 are the results based on five independent experiments. Each sample was also evaluated three times in the before mentioned Coulter Counter.

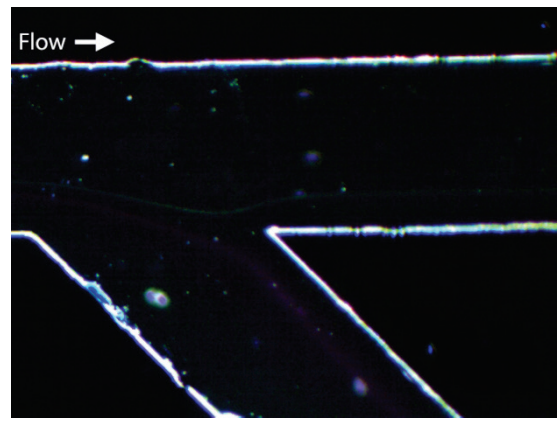

Figure 17 - Separated particle streams shown at the outlet. Red particles going downwards are the smaller (3μm) particles while the white particles continuing horisontally have a larger radius of 7μm. [a]

The separation of three micrometer particles shows good and stable results at about 95% separation efficiency. The seven micrometer particles however, are a different story. As the extremely large standard deviation indicates only a few particles (about 20 to 100 compared to around 10^4 in the case of 3 μm particles) were detected in the analyzed volume of 2 ml causing these numbers to be very unreliable. A positive indication though was that the samples where most number of particles were found also had the best separation ratio. During the experiments visual inspection (as seen in figure 8.1) showed no major separation deviations to explain the low number of particles. At this point there were a few possible explanations. An error might have occurred in the chip itself. Also something might have happened to the samples while waiting for analysis though this seems unlikely as they were stored in carefully closed tubes and thoroughly vortexed before use. To further investigate this problem the actual concentration of the original particle mix was measured using the Coulter Counter.

Table 8.1	3 μm	7 μm
Number (ml^{-1})	86,679	5,712
Volume fraction (ppm)	9.8	8.2
Mass fraction (ppm)	14.8	8.6

Table 8.1 lists the particle concentration data by number of particles, volume fraction and mass fraction. While the concentrations are almost the same, the quantity of each particle differs by a factor of 15:1. In the end the main error was found to be sedimentation in the extraction loops. The heavier 7 μm particles had time to sink and get stuck inside the tubing while the lighter 3 μm particles remained buoyant.

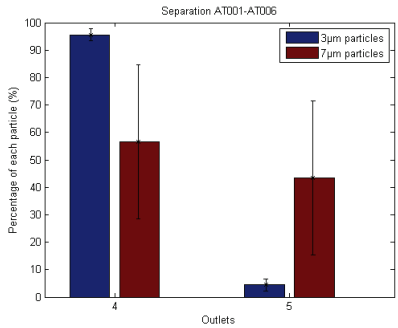

Figure 18 - Results from initial experiments separating two particles (3µm and 7µm). While the 3µm particles show good separation the results of the 7µm separation is abysmal, probably due to mishandling of extraction loops and possible too low particle concentration. [a]

This issue was remedied mainly by stirring the loops before extraction. Still, the number of 7 µm particles might have been too low to adequately detect after losses during separation, in sample transfer and storage. Additionally samples are greatly diluted for the Coulter Counter analysis.

To follow up on these problems a new particle mixture was made, now with 3, 7 and 10 µm particles and the concentrations measured beforehand. The new mixture, seen in table Table 8.2, was made to have a more balanced composition. Setup tubing and the sample collection protocol were also altered to minimize sedimentation.

Table 8.2	3 µm	7 µm	10 µm
Number (ml^{-1})	31,192	8,174	4,060
Volume fraction (ppm)	3.53	11.74	17.01
Mass fraction (ppm)	5.33	12.33	25.68

A series of four new experiments were made with the new particle mixture and the results are presented in figure 8.3. Particle flow rate was 10 µl/min and the total flow was 160 µl/min. Extraction pumps were set each run to optimally capture each particle stream. During runs the chip temperature was 30-35°C. Again each sample was examined three times in the Coulter Counter. The separation is well established with an average separation efficiency of 78.1% of 3 µm, 70.5% of 7 µm and 94.7% of 10 µm particles in the intended outlet. Though standard deviation remains rather high.

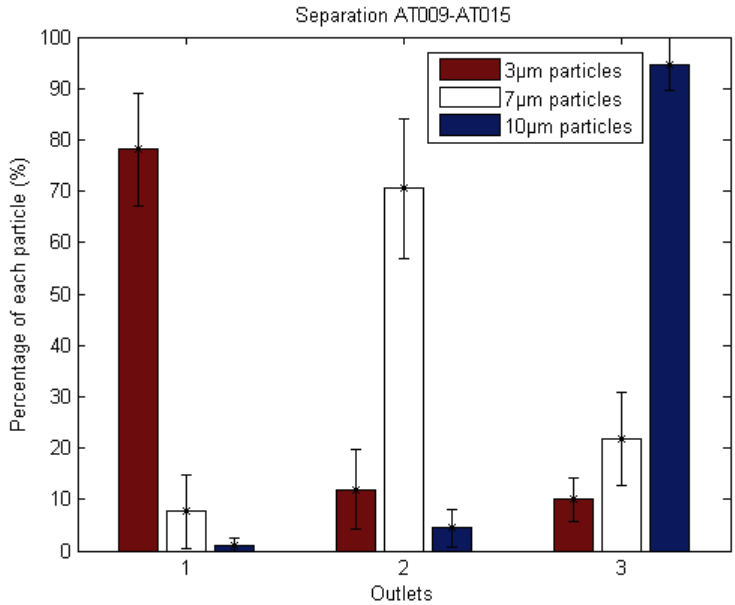

Figure 19 - Results from separation experiments involving three particles (3, 7 and 10µm). [a]

9 Discussion

9.1 Overview of Results

In a complex system like FFA the optimisation possibilities are seemingly endless. The issue of finding good settings becomes even more difficult because many influencing factors are coupled and/or are not fully investigated. In this discussion an attempt is made to give an overview of the most crucial or fundamental of these factors for future advancement of the FFA technology.

Table 9.1	3 μm	7 μm	10 μm
Petersson FFA	87%	76%	93%
Grenvall FFA (w/o prefocus)	95%	74%	84%
Grenvall FFA (w. prefocus)	97%	93%	99%
Glass FFA	78.1%	70.5%	94.7%

The separation efficiencies from experiments shown in chapter 0 are on par with previous works on FFA, all presented in table 9.1. Compared to the original (silicon based) FFA made by Petersson et al.[2] the glass FFA presented herein reaches very similar results as does it to the FFA presented by Grenvall et al.[3] (used without prefocus).

9.2 Separation flaws

Errors causing separation flaws can be classified in several different ways. One method would be to directly sort errors depending on origin (i.e. acoustic, flow oscillation etc.). I have instead decided to look at the problems from their effect. Separation errors can thus be attributed to flow fluctuations, broadening and natural variations.

Microfluidic systems are very sternly controlled so the effect natural variations ought to be minimal. As shown in chapter 3.3.1 the chip used in this thesis has well developed laminar flows (and bordering on creeping flows); hence the main degeneratory natural effect comes from diffusion. The distance traveled by particles due to diffusion is in the order of tenths of micrometers (chapter 7.1) during their time in the channel. Thus the influence of diffusion on the results seen should be negligible.

Flow errors are a more serious complication. Similar to electric circuits (as discussed in chapter 3.3.4) the pressure of different nodes will direct the current or flow. FFA-chips are run, like most microfluidic systems, with direct pressure sources so any instability in the pressure source (e.g. from a step motor) will cause deviation of the intended flow lines. Even worse, if an oscillating source such as an air bubble comes into any part of the channels, valves or syringes it will introduce those oscillations to

the entire system due to the laminar flow. Unstable flows remained a constant trouble during the experiments. While the measures (such as filling the system with liquid before runs, using more narrow tubing etc.) described in the experiment setup and results chapters did help alleviate the problem somewhat, several experiments had to be abandoned or restarted due to flow oscillation from air bubbles or other (sometimes unknown) causes. Issues surrounding flow control needs to be addressed, through equipment choices and good protocols, by anyone setting up a microfluidic system.

In addition optimisation of the flow settings should be considered. The sample to sheath flow ratio affects several factors simultaneously. Partly the throughput needs to be matched to the focusing capacity of the acoustic force. On the other hand the sample to sheath flow ratio also influences the size of the particle band as it enters the separation channel and thus also has an impact on broadening (discussed below). In my experiments the final flow ratios used were based purely on feeling from previous testing. Though this issue is not the most crucial one improvements can surely be made.

Good separation is much dependent on small particle bands. A broad band gives a higher risk of particles spilling over to neighboring outlets. Also there is the consideration of particle velocity and acoustic force. As discussed in chapter 3.3.4 the velocity varies in different parts of the channel cross-section and this is the main reason it is desirable to have a uniform particle origin in FFA. Particles positioned at different horisontal position will travel at somewhat different speed. More influential however, is the vertical position. A particle close to the ceiling or bottom of the channel will travel considerably slower than one just a few particle radii further in[64] and therefore reach the channel centerline at an earlier stage (along the channel length). Thus the prefocus, particularly the vertical focus, of the particles is of utmost importance to the separation result. This is something which could definitely have been in the experiments. The vertical focus was only roughly adjusted by visual inspection, made difficult as it concerns the depth of the channel. As long as the human eye is relied on this will remain an issue; a sensor which could evaluate the quality of the vertical (as well as horisontal) focus and adjust settings by feedback would be a great asset and a good step towards automated μTAS.

Two built-in considerations should be mentioned in connection with broadening. There is a natural limit to how small the particle band can become as the particles themselves take up space. Though I do not believe this is yet any limiting factor, especially not in the FFA presented in this thesis. Another matter is the size distribution of the particles. Manufactured particles actually always have a distribution of sizes around the specified radius. This becomes even more of an issue

with cells or other biological particles that naturally have a very broad variation. In such cases the FFA will create a continuous gradient of particle sizes.

9.3 Alternative Chip Design

A drawback of the basic chip design (and most microfluidic applications) is the need of pumps. Particularly if all or all but one inlet as well as outlet must be controlled individually which is the case with an FFA-chip. Also the sheath flow described in chapter 6.1 creates the need of additional pumps. A possible solution to avoid this extra inlet could be self lamination through flow splitting and recombination[33]; this would however significantly increase the total chip area possibly reducing effective energy transfer from the piezo-electric actuators. Instead an alternate chip design is suggested (figure 9.1) where the particle flow is first focused at the chip's basic frequency. The particle stream then continues into a separation channel twice as wide as the prefocus channel. Two pressure nodes will be present and particles will now go towards either one. Due to the symmetry of the flow both particle lines can be extracted through a single outlet with a "diamond shape" design.

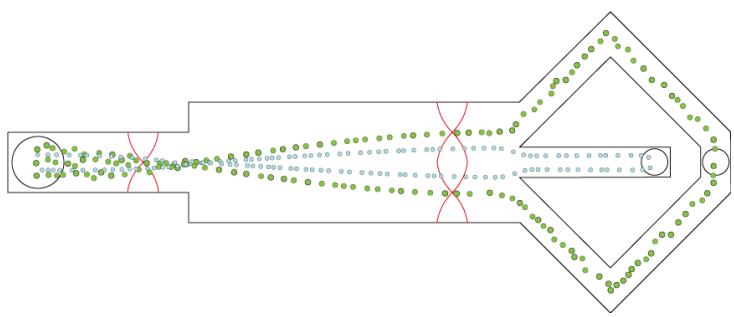

Figure 20 - Illustration of the alternative FFA design. By having a separation channel with double width in respect to the prefocus channel only one transducer needs to be used. With this design the fraction of the smallest particles will be collected in the middle while larger particles continue. [a]

Additional identical chips can be added sequentially, each extracting a fraction of the smallest particles present. A modular design of this kind has great advantages because of its flexibility and can be made either by combining separate chips or preferably by integrating on a single wafer as seen in figure 9.2. Also each new module would add an equal amount of fluidic resistance opening up for the possibility of a geared syringe pump with only one motor.

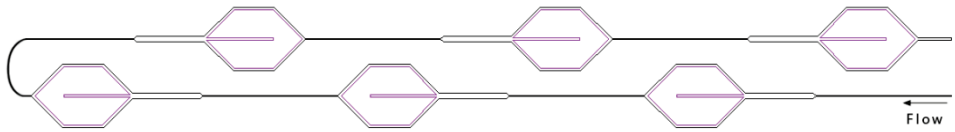

Figure 21 - A benefit of the alternative design is the possibility of arranging a serial setup. Each unit collects the smallest fraction remaining. [a]

10 Conclusions

In this thesis a thorough overview of the FFA technology is made together with the investigation of a possible glass FFA design.

Background theory is presented both for microchip fabrication as well as fluidics and ultrasound physics. The microchip fabrication techniques used are kept simple to improve reproducibility and enable in-house manufacturing and testing. Existing FFA design is evaluated and altered to work with limitations of glass fabrication, particularly isotropic etching. As channels of different widths can not be used the prefocus channel is designed to match the separation channel. This enables 2D focus also in the separation channel though prefocus and separation can no longer be controlled independently by separate frequencies.

Results show that the basic glass FFA chip reaches similar results (though not ideal) as previous designs. Sensitivity is expected to increase with optimization and several parameters affecting performance have been identified. Foremost is better 2D focus but also better chip layout (though exactly what this involves is not yet fully established) and improved design so as to minimize edge effects etc. Finally an alternative design is shown addressing some of the issues inherent in the FFA technology.

The outlook for microfluidics is bright in my opinion. Medical needs creates an opening for research in this (wide) area. Eventually commercial interest will fuel the development even further. And because the field is at heart an applied one, research should focus on moving towards an end product. So far many interesting and good methods have been developed but, in my opinion, too few strive towards a true μTAS. Working not only with the principles and basic technology, but with a finished system in mind forces one to practical solutions and to actually deal with the integration complexity.

Most systems in use today utilize passive technology (such as capillary force driven flows) and it will be a major challenge for other technologies including acoustophoresis to reach the same level of both robustness and simplicity. Only time will show when dedicated products and standards in microfluidics start to emerge.

I would like to conclude by thanking you for reading all the way to the end.

おつかれさまでした！

11 Populärvetenskaplig sammanfattning

I framväxten av ”life science” och dess underområden så som genomik, proteomik och medicinteknik ökar behovet av ny teknologi för att analysera och behandla prover i alla dess former. En sådan ny teknik är *Free Flow Acoustophoresis* (FFA) som använder ultraljud till att sortera olika slags partiklar i vätskor beroende på storlek. På LTH finns ett starkt arv efter Helmuth Hertz och Inge Edler som var pionjärer inom diagnostiskt ultraljud. Idag har forskningen fortsatt och breddats till att omfatta en mängd områden och applikationer samtidigt som få blivande mammor skulle välja att inte undersöka sina barn med ultraljud. Medicinskt sett är det en enkel, flyttbar och billig metod att använda. Men framför allt är ultraljud en metod som inte påverkar det som undersöks, en mycket viktig faktor både inom medicin som i vetenskapliga experiment.

Icke-invasiviteten gäller även på mikro- och nanoskala där ultraljud kan användas för att flytta på celler och andra former av partiklar utan att skada dem. I denna rapport visas tillverkningen och bruket av chip med mikroskopiska kanaler vari vätskor med partiklar kan ledas. Genom att lägga ett stående ultraljudsfält över en vätskefylld kammare med partiklar (likt en resonanslåda på en gitarr) kommer partiklarna påverkas av en akustisk kraft. Denna kraft kan antingen användas till att hålla partiklar på plats eller till att flytta dem utifrån kammarens utseende, vätskans flöde och andra kringliggande faktorer. Kraften som påverkar partiklarna (och därmed även deras hastighet) kommer att vara beroende på radien vilket kan utnyttjas till att sortera ut partiklarna efter storlek.

Detta är den princip som används i FFA. Partiklarna leds in i en rak kanal där kraften från ultraljudet fokuserar partiklarna till mitten så att de lägger sig på rad. Nästa steg är att det kommer in ett styrflöde från sidan som pressar ut partiklarna till ena kanten. Därefter kommer de åter igen börja åka in mot mitten. Men nu är partiklarnas hastighet proportionell mot deras storlek varvid de stora partiklarna kommer att nå mitten först och övriga i successivt långsammare takt. Därmed uppstår band av de olika storlekarna som kan ledas ut genom varsitt utlopp för vidare undersökning.

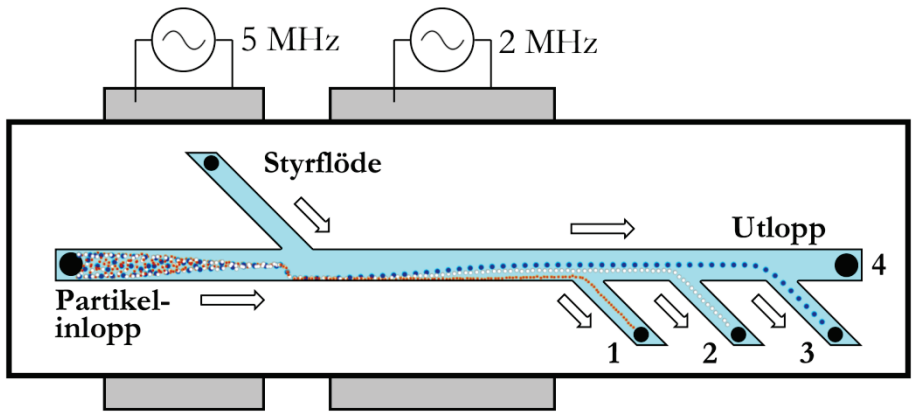

Figur 1 – De blandade partiklarna kommer in genom partikelinloppet till förfokuseringskanalen på vänster sida. Partiklarna fortsätter vandra i kanalen och fokuseras under tiden till mitten av kanalen genom den akustiska kraften. Ett styrflöde pressar sedan ut alla partiklar till kanten varefter de börjar vandra in mot mitten igen. Men nu är deras hastighet storleksberoende där större partiklar flyttar sig snabbare. Därför uppstår en delning mellan olika storlekar och med rätt anpassade flödeshastigheter kan de olika partikeltyperna ledas ut genom olika utlopp.

Ett par exempel på områden där FFA-tekniken kan användas är:

- Undersökning av hur mediciner påverkar celler i olika stadier. Beroende på var i sin livscykel en cell befinner sig (om den precis på väg att dela sig eller jobbar med att producera proteiner till kroppen) har cellen olika storlek. Därför går det att tillsätta en medicin till en cellpopulation och sedan sortera den efter storlek med hjälp av FFA-tekniken. Det går då att se hur celler i olika stadier svarar på en och samma dos av en medicin.
- Ett annat exempel där FFA-tekniken kan komma till användning är i partikeltillverkning. Med hjälp av separationen kan undergrupper av storlekar väljas ut för att möta mer exakta specifikationer från kunder.

En viktig fråga är valet av material som FFA:n byggs i. Huvudfokus i rapporten är hur metoden kan överföras från ett kiselbaserat chip till glas. Traditionellt sett tillverkas mycket mikromekaniska och mikrofluidiska produkter i kisel med all den kunskap och de processtekniker som kommer från industrin för integrerade kretsar. Men glas har många fördelar som gör det attraktivt som basmaterial. Kemister har under flera hundratals år använt glas på grund av dess transparens, värmestabilitet och att det inte reagerar med de flesta ämnen. Glas är också billigare och produktionen av en kommersiell produkt kan enklare anpassas till storskalig produktion. I rapporten visas att FFA-tekniken kunnat anpassas till glaschip och att separationseffektiviteten hos dessa är jämförbar med motsvarande kiselbaserade chip.

12 Popular Science Summary

In the growth of the life science field and its subareas such as genomics, proteomics and biomedicine the need for new technologies to analyse and treat samples is increasing. One such new technology is Free Flow Acoustophoresis (FFA) which utilizes ultrasound to sort particles differentiated by size. The technical faculty of Lund University (Sweden) has a strong heritage from Helmuth Hertz and Inge Edler who together where pioneers of diagnostic ultrasound. Today their research has continued and broadened to include numerous areas and applications at the same time as few mothers to be would choose not to do ultrasonic investigation. Medically ultrasound is a simple, portable and cheap tool to use. But most of all it is a method that does not affect the subject of measurement, a very important factor in medicine as well as in scientific experiments.

The non-invasiveness is also valid in the micro and nano domain where ultrasound can be used to move cells and other forms of particles without damaging them. In this report the manufacture and use of chips with microscopic channels is shown. These channels can be used to lead fluids with suspended particles. By creating a standing wave of ultrasound over a fluid chamber (similar to the resonance box of a guitar) any particles present will be affected by an acoustic force. This force can be used either to keep particles in place or to move them in a manner decided by the shape of the chamber, fluid flows and other related factors. If particles are moved their speed will depend on radii which can be used to separate them according to size.

This is the principle used in FFA. Particles are taken into a straight channel where the acoustic force focuses the particles into the middle so that they form a thin line. In the next step a side flow pushes the particles to one side. After this the particles will again start to move towards the middle. But now the particle velocity is proportional to their size with the effect that large particles will reach the middle first and smaller ones successively at slower rate. By tuning fluid flow and time the differently sized particles can be lead into separate outlets for further investigation or treatment.

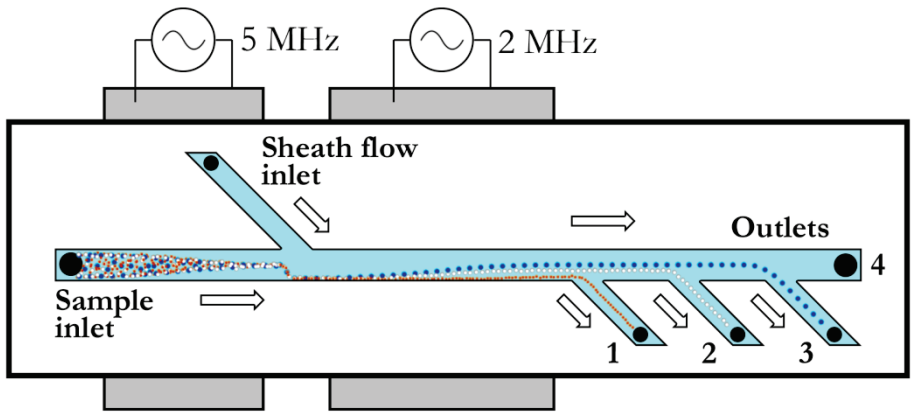

Figure 1 – The mix of particles enters through the sample inlet into the prefocus channel. In the prefocus channel the particles are focused to the center by the acoustic force. Particles are then pushed towards the wall by a sheath flow as they enter the separation channel. In this part of the chip the particles will again start moving towards the center. But as their speed is determined by size, where larger particles move faster, dispersion between particles will arise. With appropriately adjusted flow speeds the different particles can be extracted through different outlets.

A few examples applications of the FFA technology:

- Investigating how cells at different stages in the cell cycle responds to a medicine. Depending on its life cycle position (if it is producing proteins for the body or ready to divide) a cell has different size. FFA technology can thus be used to separate cells after drug administration. The concentration delivered to each cell is then certainly the same.
- Another example when FFA technology could prove useful is during particle manufacturing. With the help of separation subgroups of sizes can be chosen to better meet customer specifications.

Another important issue is the choice of material for the FFA microfluidic chip. The main focus of the thesis is how the method can be transferred from a silicon based chip to a glass based chip. Traditionally many micromechanical and microfluidic devices are made from silicon due to the knowledge and vast number of process methods available from integrated circuit technology. But glass has many advantageous properties. Chemists have for hundreds of years used glass because of its transparency, thermal stability and inertia (ability to *not* react). Glass is also cheaper than silicon and fabrication can more readily be adjusted to large scale production. Plastics are another set of materials used in microfluidic devices though due to the high attenuation of sound plastics are unsuitable materials in ultrasound applications. In the thesis it is shown that the FFA technology can be adjusted to glass based chips and that the separation efficiency matches corresponding silicon based chips.

13　非専門家向けの概要

生命科学やその一部であるゲノム科学、プロテオーム解析、生物医学等が発展するにつれ、サンプルを分析したり取り扱ったりするための新しい技術の必要性も増えてきた。大きさの異なる分子を超音波を使って分離する、フリーフロー音波泳動（Free Flow Acoustrophoresis: FFA）も、そのような新しい技術の一つである。スウェーデン、ルンド大学工学部では、超音波技術を医学的診断に先駆的に適用したヘルムット・ヘルツとインゲ・エードュラーの始めたこの分野での研究を、強く継承してきた。彼らの始めたこの研究分野は、数知れない領域において様々な形での適用が可能であり、その研究は今日も続けられ、さらに拡がっている。超音波による診断は受けないことを選択する妊婦はほとんどいないだろう。医療において、超音波装置は単純で、移動可能であり、安価な器具である。その上、診断対象に影響を与えないという、医学的にも、科学的実験においても、大変重要な特性を持ち合わせている。

この、非侵襲性という特性は、マイクロ、ナノといった、非常に小さな単位でのみ計測しうるような物体にもあてはまる。超音波を使えば、細胞やその他の形態の分子を、傷つけることなく動かすことができるのである。本論文では、肉眼で見えない大きさの導管入りチップの製造方法と使い方について述べている。こういった導管を使えば、諸分子の含まれる液体を望むところに導くことができるのである。液体の部屋（喩えていうのであれば、ギターの共鳴箱のようなものである）に超音波の定常波を起こすと、そこに存在する分子は皆、音波の力に影響されることになる。この力を利用して、分子を一定の場所にとどめておくこともできれば、部屋の形、液体の流れその他の関連因子を調節し、分子をある法則に則った形で動かすこともできる。分子の動く速度は、その半径の長さによって決まることを活用して、分子を大きさ別に分けることもできる。

これが、フリーフロー音波泳動（FFA）に使われている原則である。真っ直ぐな導管に入れられた分子は、音波の力により、導管の中央に細い線状に集中する。この導管に、別の流れを横から挿入すると、分子は片方に押される。押された分子は、再度中央に戻り始める。しかし今度は、分子の動く速度はその大きさに比例することから、まず最初に大きな分子が中央にたどりつき、追って、より小さな分子が徐々にたどりつくことになる。液体の流れや分子の導管内での活動時間を調整することによ

り、異なる大きさの分子を別々の出口に導いて分離し、それをさらに調査したり別の処理を加えたりすることができるのである（下図参照）。

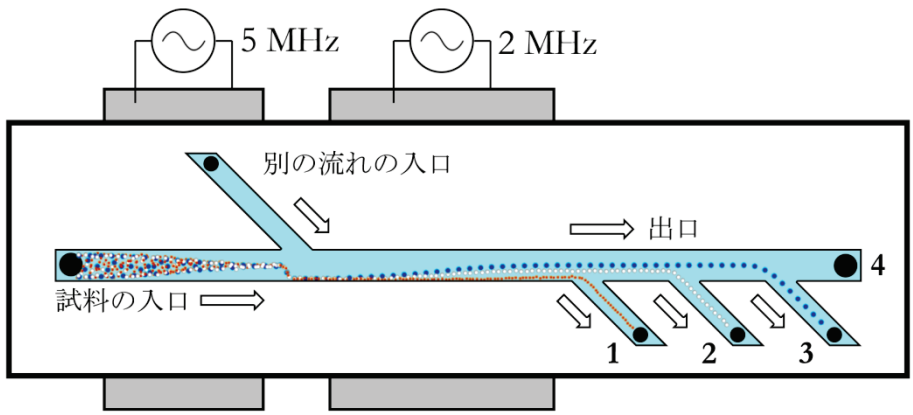

図１　導管の入り口から分子ミックスを流入する。この導管内では、分子は音波の力により中央に集められる。分子はその後、別の導管から入ってきた被覆フローによって壁側に押される。チップのこの部分では、分子はその後再び中央に動きはじめる。しかし、そのスピードは分子の大きさによって決まり、大きな分子ほど早く動くことから、分子間の分散が起こる。流れの速さを適宜調節することにより、異なる分子を異なる出口に抽出することができる。

FFA 技術の適用例としては、以下のようなものが挙げられる。

- 異なる成長過程にある細胞が、ある薬にどのように反応するかの調査。細胞の大きさは、そのライフサイクル上の成長段階（例えば、蛋白質を作り出しているのか、分裂の前か後か等）によって異なる。そこで、薬を用いた後の細胞を、FFA 技術を使って分離することができるのである。各細胞に到達した薬の濃度は確実に同じものとなる。
- 分子の製造。分離の機能を利用して、製造した分子の中から、顧客の注文に応じて、異なる大きさのグループを選ぶことができる。

FFA マイクロ流体工学のチップに使われる素材の選択も、重要である。この修士論文では主として、シリコンベースのチップからガラスベースのチップに移行するにはどうすればいいか、ということに、焦点を絞った。マイクロ力学及びマイクロ流体工学の装置は、集積回路技術の分野に存在するあまたの知識や製造方法故に、シリコン製であることが多かった。しかしながら、ガラスには数多くの特性がある。ガラスは、その透明性、熱安定性及び不反応性といった特性から、何百年もの間化学者に使われてきた。また、ガラスはシリコンより安く、製造方法としても大規模生産に馴染みやすい。マイクロ流体工学では、プラスチックも素材として使われているが、音を希薄化させることから、超音波の適用には適さない。論文では、FFA 技術はガラスベースのチップにも適用することができ、その分別効率は、同様のシリコンベースのチップに匹敵することを示した。

References

1. Petersson, F. On acoustic particle and cell manipulation in microfluidic systems. (2007).

2. Petersson, F., Åberg, L., Swärd-Nilsson, A.-M. & Laurell, T. Free Flow Acoustophoresis: Microfluidic-Based Mode of Particle and Cell Separation. *Analytical Chemistry* **79**, 5117–5123 (2007).

3. Grenvall, C., Augustsson, P. & Laurell, T. Reduced particle size dispersion in free flow acoustophoresis using 2D acoustic prefocusing. 3 (2009).

4. Fakta - Region Skåne. at <http://www.skane.se/sv/Webbplatser/Labmedicin_Skane/Vansterspalt/Fakta/>

5. Region Skånes budget 2012 - Region Skåne. at <http://skane.se/sv/Demokrati/Budget/Region-Skanes-budget-2012/>

6. Palais, R. π is wrong! *The Mathematical Intelligencer* **23**, 7–8 (2001).

7. Hartl, M. The Tau Manifesto. (2011).at <http://tauday.com/>

8. Evander, M. *et al.* Noninvasive Acoustic Cell Trapping in a Microfluidic Perfusion System for Online Bioassays. *Analytical Chemistry* **79**, 2984–2991 (2007).

9. Evander, M. Cell and particle trapping in microfluidic systems using ultrasonic standing waves. (2008).

10. Takahashi, M., Sugimoto, K. & Maeda, R. Nanoimprint of Glass Materials with Glassy Carbon Molds Fabricated by Focused-Ion-Beam Etching. *Jpn. J. Appl. Phys.* **44**, 5600–5605 (2005).

11. Takahashi, M., Murakoshi, Y., Maeda, R. & Hasegawa, K. Large area micro hot embossing of Pyrex glass with GC mold machined by dicing. *Microsyst Technol* **13**, 379–384 (2006).

12. Sze, S. M. *Semiconductor Devices: Physics and Technology*. (Wiley: 2002).

13. Sze, S. M. *Semiconductor Devices: Physics and Technology*. (Wiley: 2002).

14. Madou, M. *Fundamentals of Micro Fabrication*. (CRC Press: Florida, USA, 1997).at <http://www.crcpress.com/microfab>

15. Sze, S. M. *Semiconductor Devices: Physics and Technology*. (Wiley: 2002).

16. Steinsland, E. *et al.* Boron etch-stop in TMAH solutions. *Sensors and Actuators A: Physical* **54**, 728–732 (1996).

17. Palm, L. Development and characterization of silicon micromachined nozzle units for continuous ink jet printers. (1998).at <http://cat.inist.fr/?aModele=afficheN&cpsidt=951907>

18. Palm, L., Laurell, T. & Nilsson, J. Development and Characterisation of Silicon Nozzle Arrays for Continuous Ink Jets. (1999).

19. Raley, N. F. Examination of glass-silicon and glass-glass bonding techniques for microfluidic systems. *Proceedings of SPIE* 40–45 (1995).doi:10.1117/12.221298

20. Nguyen, N.-T. & Wereley, S. T. *Fundamentals and Applications of Microfluidics*. (Artech House: 2006).

21. Jia, Z.-J., Fang, Q. & Fang, Z.-L. Bonding of Glass Microfluidic Chips at Room Temperatures. *Analytical Chemistry* **76**, 5597–5602 (2004).

22. Allen, P. B. & Chiu, D. T. Calcium-Assisted Glass-to-Glass Bonding for Fabrication of Glass Microfluidic Devices. *Analytical Chemistry* **80**, 7153–7157 (2008).

23. Iles, A., Oki, A. & Pamme, N. Bonding of soda-lime glass microchips at low temperature. *Microfluid Nanofluid* **3**, 119–122 (2006).

24. Terry, S. C., Jerman, J. H. & Angell, J. B. A gas chromatographic air analyzer fabricated on a silicon wafer. *IEEE Transactions on Electron Devices* **26**, 1880– 1886 (1979).

25. Whitesides, G. M. The origins and the future of microfluidics. *Nature* **442**, 368–373 (2006).

26. Nguyen, N.-T. & Wereley, S. T. *Fundamentals and Applications of Microfluidics*. (Artech House: 2006).

27. Little, J. & Lee, B. *Bruce Lee: A Warrior's Journey*. (2001).

28. Sharp, K., Adrian, R. J., Santiago, J. G. & Molho, J. I. Liquid Flows in Microchannels. *The MEMS Handbook* 1–17 (2002).

29. Lenshof, A. Acoustic standing wave manipulation of particles and cells in microfluidic chips. (2009).

30. Bruus, H. Acoustofluidics. *Theoretical Microfluidics* **1**, 25–31 (2008).

31. Dusenbery, D. B. *Living at Micro Scale: The Unexpected Physics of Being Small*. (Harvard University Press: 2009).

32. Takagi, J., Yamada, M., Yasuda, M. & Seki, M. Continuous particle separation in a microchannel having asymmetrically arranged multiple branches. *Lab Chip* **5**, 778 (2005).

33. Yamada, M. & Seki, M. Microfluidic Particle Sorter Employing Flow Splitting and Recombining. *Analytical Chemistry* **78**, 1357–1362 (2006).

34. Bruus, H. Microfluidics and ultrasound acoustophoresis. (2010).

35. Lauga, E., Brenner, M. P. & Stone, H. A. Microfluidics: The no-slip boundary condition. *cond-mat/0501557* (2005).at <http://arxiv.org/abs/cond-mat/0501557>

36. Nguyen, N.-T. & Wereley, S. T. *Fundamentals and Applications of Microfluidics*. (Artech House: 2006).

37. Nguyen, N.-T. & Wereley, S. T. *Fundamentals and Applications of Microfluidics*. (Artech House: 2006).

38. Ursell, T. S. The Diffusion Equation: A Multidimensional Tutorial. (2007).

39. Einstein, A. On the movement of small particles suspended in stationary liquids required by the molecular kinetic theory of heat. *Annalen der Physik* 549–560 (1905).

40. Batchelor, G. K. Flow due to a moving body at small Reynolds number. *An introduction to fluid dynamics* 229–233 (1967).

41. Batchelor, G. K. Flow due to a moving body at small Reynolds number. *An introduction to fluid dynamics* 234 (1967).

42. Jönsson, G. & Nilsson, E. Våglära och Optik. *Våglära och Optik* 43 (2002).

43. Bruus, H. Acoustofluidics. *Theoretical Microfluidics* **1**, 255–274 (2008).

44. Smart, L. E. & Moore, E. A.*Solid State Chemistry: An Introduction, Third Edition* 331–333 (2005).

45. Hoskins, P. Transducers and Beam-forming. *Diagnostic ultrasound : physics and equipment* 23–48 (2003).

46. Evander, M. *Cell and Particle Trapping in Microfluidic Systems Using Ultrasonic Standing Waves*. (Lund University: 2008).at <http://lup.lub.lu.se/record/1149123>

47. King, L. V. On the Acoustic Radiation Pressure on Spheres. *Proceedings of the Royal Society of London. Series A - Mathematical and Physical Sciences* **147**, 212 –240 (1934).

48. Gor'kov, L. P. On the Forces Acting on a Small Particle in an Acoustical Field in an Ideal Fluid. (1962).at <http://adsabs.harvard.edu/abs/1962SPhD....6..773G>

49. Coakley, W. T. Ultrasonic separations in analytical biotechnology. *Trends Biotechnol* **15**, 506–511 (1997).

50. Yoshioka, K. & Kawashima, Y. Acoustic radiation pressure on a compressible sphere. *Acustica* **5**, 167–173 (1955).

51. Petersson, F., Nilsson, A., Holm, C., Jönsson, H. & Laurell, T. Separation of lipids from blood utilizing ultrasonic standing waves in microfluidic channels. *Analyst* **129**, 938 (2004).

52. Gröschl, M. Ultrasonic Separation of Suspended Particles - Part I: Fundamentals. *Acta Acustica united with Acustica* **84**, 432–447 (1998).

53. Petersson, F. *On acoustic particle and cell manipulation in microfluidic systems*. (Department of Electrical Measurements Lund Institute of Technology Lund University: Lund, 2007).

54. Hammarström, B., Laurell, T. & Nilsson, J. Seed particle-enabled acoustic trapping of bacteria and nanoparticles in continuous flow systems. *Lab Chip* **12**, 4296–4304 (2012).

55. Hertz, T. G. Applications of Acoustic Streaming. (1993).

56. Nyborg, W. L. Acoustic Streaming. *Nonlinear acoustics* 207–228 (1998).

57. Rayleigh, B. J. W. S. & Lindsay, R. B. *The theory of sound*. (Courier Dover Publications: 1877).

58. Bengtsson, M. & Laurell, T. Ultrasonic agitation in microchannels. *Analytical and Bioanalytical Chemistry* **378**, 1716–1721 (2004).

59. Alberts, B. *et al.Essential Cell Biology, Second Edition* 329–330 (2003).

60. Iacopini, S. & Piazza, R. Thermophoresis in protein solutions. *Europhys. Lett.* **63**, 247–253 (2003).

61. Shi, J. *et al.* Three-dimensional continuous particle focusing in a microfluidic channel via standing surface acoustic waves (SSAW). *Lab Chip* **11**, 2319 (2011).

62. Oxley, J. & Smith, J. PEROXIDE EXPLOSIVES. *Detection and Disposal of Improvised Explosives* 113–121 (2006).at <http://www.springerlink.com/content/62g84165l1h6874/>

63. Oxley, J. C., Smith, J. L., Shinde, K. & Moran, J. Determination of the Vapor Density of Triacetone Triperoxide (TATP) Using a Gas Chromatography Headspace Technique. *Propellants, Explosives, Pyrotechnics* **30**, 127–130 (2005).

64. Augustsson, P. & Lunds tekniska högskola, *On Microchannel Acoustophoresis: Experimental Considerations and Life Science Applications* 18–20,28–30 (2011).

Figure references

[a] Figure 2.1 - By the author.
[a] Figure 2.2 - By the author.
[a] Figure 3.1 - By the author
[b] Figure 3.2 - Google maps, decimal degrees: 69.472005,-25.167389, Terrametrics mapdata, Google inc., 2012-10-18
[a] Figure 3.3 - By the author
[c] Figure 4.1 - Lenshof A, Acoustic standing wave manipulation of particles and cells in microfluidic chips, LTH, Sweden, 2009
[a] Figure 5.1 - By the author.
[a] Figure 5.2 - By the author.
[a] Figure 5.3 - By the author.
[d] Figure 5.4 - Evander M, Cell and particle trapping in microfluidic systems using ultrasonic standing waves, LTH, Sweden, 2008.
[d] Figure 5.5 - Evander M, Cell and particle trapping in microfluidic systems using ultrasonic standing waves, LTH, Sweden, 2008.
[e] Figure 6.1 - Peterson F, On acoustic particle and cell manipulation in microfluidic systems.
[f] Figure 6.2 - Grenvall C, Reduced particles size dispersion in free flow Acoustophoresis using 2D acoustic prefocusing, LTH, Sweden, 2009.
[a] Figure 7.1 - By the author.
[a] Figure 7.2 - By the author.
[a] Figure 7.3 - By the author.
[a] Figure 8.1 - By the author.
[a] Figure 8.2 - By the author.
[a] Figure 8.3 - By the author.
[a] Figure 9.1 - By the author.
[a] Figure 9.2 - By the author.